

Tilings of the sphere by congruent regular triangles and congruent rhombi*

Qi Yuan¹, Erxiao Wang²

Abstract All edge-to-edge tilings of the sphere by congruent regular triangles and congruent rhombi are classified as: (1) a 1-parameter family of protosets each admitting a unique $(2a^3, 3a^4)$ -tiling like a triangular prism; (2) a 1-parameter family of protosets each admitting 2 different $(8a^3, 6a^4)$ -tilings like a cuboctahedron and a triangular orthobicupola respectively; (3) a sequence of protosets each admitting a unique $(2a^3, (6n - 3)a^4)$ -tiling like a generalized anti-triangular prism for each $n \geq 3$; (4) 26 sporadic protosets, among which nineteen admit a unique tiling, one admits 3 different tilings, one admits 5 different tilings, three admit 2 different tilings, two admit too many tilings to count. The moduli of parameterized tilings and all geometric data are provided.

Keywords spherical tiling, prototile, protoset, regular triangle, rhombus, classification.

2000 MR Subject Classification 52C20, 05B45

1 Introduction

In recent years, all edge-to-edge monohedral tilings of the sphere by congruent simple polygons (assuming the degree of all vertices ≥ 3) have been fully classified after many authors' efforts, see [12, 13, 11, 14, 15, 16, 3, 8, 9, 10, 5]. Multihedral tilings of the sphere by regular polygons have just been classified in both edge-to-edge and non-edge-to-edge cases, see [2]. However, multihedral tilings of the sphere by general polygons are rarely studied.

In this paper, we will start the study of edge-to-edge dihedral tilings of the sphere by congruent triangles and congruent quadrilaterals, and fully classify the equilateral case. In other words, we classify edge-to-edge tilings of the sphere by congruent regular triangles and congruent rhombi (see Fig.1) with edge lengths a , and all vertices have degree ≥ 3 . We will simply call such tilings (a^3, a^4) -tilings. We also denote the angle of the regular triangle by α and denote the angles of the rhombus by β, γ . Without loss of generality, we assume that $\beta \geq \gamma$.

We use $\alpha^k \beta^l \gamma^m$ to mean a vertex having k copies of α , l copies of β , etc. The *anglewise vertex combination*, abbreviated as **AVC**, is the collection of all vertices in a tiling. Then the notation $T(2a^3, 3a^4; 6\alpha\beta\gamma)$ means the tiling has exactly 2 regular triangles, 3 rhombi and 6 vertices $\alpha\beta\gamma$, and is uniquely determined by them. In general there may exist several different tilings with the same set of vertices. Then we use $\{8a^3, 6a^4; 12\alpha^2\beta\gamma : 2\}$ to mean that there are 2 different tilings.

¹School of Mathematical Sciences, Zhejiang Normal University, Jinhua, Zhejiang Province, 321004, China. E-mail: qiyuan@zjnu.edu.cn

²Corresponding author. School of Mathematical Sciences, Zhejiang Normal University, Jinhua, Zhejiang Province, 321004, China. E-mail: wang.eric@zjnu.edu.cn

*Research was supported by Key projects of Zhejiang Natural Science Foundation No. LZ22A010003 and ZJNU Shuang-Long Distinguished Professorship Fund No. YS304319159.

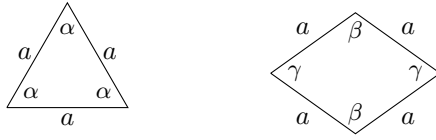


Figure 1: The regular triangle and the rhombus.

The icosahedron naturally gives a monohedral tiling $T(20a^3; 12\alpha^5)$, in which any two adjacent regular triangles can be merged into a rhombus *i.e.* $\beta = 2\alpha = 2\gamma$ that produces some (a^3, a^4) -tilings. We will call all such (a^3, a^4) -tilings to be of the **icosahedral type**. We also have the **octahedral type** (the tetrahedral type is dismissed since it has vertices of degree 2).

The very useful tool *adjacent angle deduction* (abbreviated as **AAD**) has been introduced in [14, Section 2.5]. We give a quick review here using Figure 2. Let “|” denote an a -edge. Then we indicate the arrangements of angles and edges by denoting the vertices as $|\alpha|\alpha|\beta|\beta|$ or $|\alpha|\beta|\alpha|\beta|$. The notation can be reversed, such as $|\alpha|\alpha|\beta|\beta| = |\beta|\beta|\alpha|\alpha|$; and it can be rotated, such as $|\alpha|\alpha|\beta|\beta| = |\alpha|\beta|\beta|\alpha|$. We also denote the first vertex in Figure 2 as $|\beta|\beta|\dots$, $|\beta|\beta|\dots$, $|\alpha|\beta|\dots$, $|\alpha|\beta|\dots$, and denote the consecutive angle segments as $|\beta|\beta|$, $|\beta|\beta|$, $|\alpha|\beta|$, $|\alpha|\beta|$.



Figure 2: Different Adjacent Angle Deductions of $\alpha^2\beta^2$.

We write ${}^\lambda\theta^\mu$ to mean λ, μ are the two angles adjacent to θ in a tile. The first picture has the AAD $|\alpha\alpha\alpha|\alpha\alpha|\gamma\beta\gamma|\gamma\beta\gamma|$, which gives $|\alpha|\alpha|\alpha|\dots$, $|\alpha|\gamma|\dots$, $|\gamma|\gamma|\dots$; the second has the AAD $|\alpha\alpha\alpha|\gamma\beta\gamma|\alpha\alpha|\gamma\beta\gamma|$, which gives $|\alpha|\gamma|\dots$.

Let f_Δ, f_\diamond be the numbers of triangle tiles and quadrilateral tiles; S_Δ, S_\diamond be the areas of triangle tiles and quadrilateral tiles. We have $f_\Delta S_\Delta + f_\diamond S_\diamond = 4\pi$ (the radius of the sphere is always 1).

Theorem. *All (a^3, a^4) -tilings are classified as:*

1. *A 1-parameter family of protosets each admitting a unique tiling $T(2a^3, 3a^4; 6\alpha\beta\gamma)$ like a triangular prism. (See the 1st of Fig. 3);*
2. *A 1-parameter family of protosets each admitting 2 different tilings $\{8a^3, 6a^4; 12\alpha^2\beta\gamma : 2\}$ like a cuboctahedron and a triangular orthobicupola respectively. All $\alpha^2\beta\gamma$ vertices are $|\alpha|\beta|\alpha|\gamma|$ in the first tiling. By flipping half of the first, we get the second tiling which has six $|\alpha|\alpha|\beta|\gamma|$ near the equator. (See the 2nd and 3rd of Fig. 3);*
3. *A sequence of protosets each admitting a unique tiling $T(2a^3, (6n - 3)a^4; 6\alpha\beta\gamma^n, (6n - 6)\beta^2\gamma)$ like a generalized anti-triangular prism for each $n \geq 3$. (See the 4th, 5th and 6th of Fig. 3 when $n = 3, 4, 5$);*
4. *Twenty-six sporadic protosets as listed in Table 1, among which nineteen admit a unique tiling, one admits 3 different tilings, one admits 5 different tilings, three admit 2 different tilings, two admit too many tilings to count.*

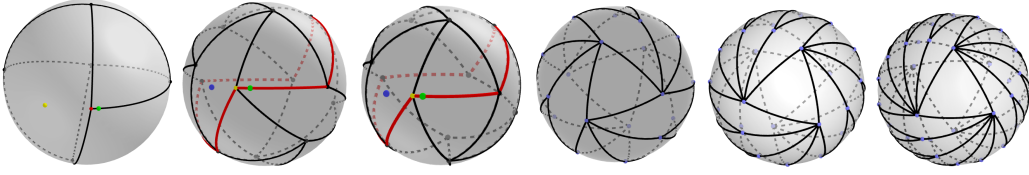


Figure 3: Some 3D pictures in the first, second and third classes.

(f_Δ, f_\diamond)	Page	$\alpha, \beta, \gamma; a$	all vertices & tilings
(4,1)	9	$\frac{1}{2}, 1, \gamma = \beta; \frac{1}{2}$	$4\alpha^2\beta, 1\alpha^4$
(6,3)		$\frac{1}{2}, 1, \frac{1}{6}; \frac{1}{2}$	$6\alpha^2\beta, 2\alpha^3\gamma^3$
(4,4)		$\frac{1}{2}, 1, \frac{1}{4}; \frac{1}{2}$	$4\alpha\beta\gamma^2, 4\alpha^2\beta$
(6,2)		$\frac{1}{2}, 1, \frac{1}{4}; \frac{1}{2}$	$4\alpha^2\beta, 2\alpha^3\gamma^2, 1\alpha^4$
(4,2)		$\frac{1}{2}, 1, \frac{1}{2}; \frac{1}{2}$	$4\alpha^2\beta, 2\alpha^2\gamma^2$
(6,1)		$\frac{1}{2}, 1, \frac{1}{2}; \frac{1}{2}$	$2\alpha\beta\gamma, 2\alpha^2\beta, 2\alpha^3\gamma$ $2\alpha^2\beta, 2\alpha^3\gamma, 2\alpha^4$
(8,2)	10	0.4335, 0.6992, $\gamma = \beta$; 0.4158	$8\alpha^3\beta$
(32,6)		0.3621, 0.5513, $\gamma = \beta$; 0.2427	$24\alpha^4\beta$
(8,18)		0.3596, 0.5467, $\gamma = \beta$; 0.2326	$24\alpha\beta^3 : 2$
(4,3)	8	$\frac{4}{9}, \frac{7}{9}, \frac{2}{3}; 0.4326$	$3\alpha\beta^2, 3\alpha^3\gamma, 1\gamma^3$
(4,4)	17	0.4296, 0.7851, 0.5703; 0.4094	$4\alpha\beta^2, 4\alpha^2\gamma^2$
(8,3)	20	0.4195, 0.7412, 0.5804; 0.3918	$6\alpha^3\beta, 3\alpha^2\gamma^2$
(4,12)	13	0.3754, $\frac{2}{3}, 0.4789$; 0.2884	$12\alpha\beta\gamma^2, 4\beta^3$
(8,12)	19	0.3701, 0.6298, $\frac{1}{2}$; 0.2716	$6\alpha^2\beta^2, 12\alpha\beta\gamma^2$
(20,6)	25	0.3807, 0.8578, 0.2385; 0.3040	$12\alpha^3\beta, 6\alpha^4\gamma^2$
(8,24)	17	0.3541, 0.5729, $\frac{1}{2}$; 0.2082	$24\alpha\beta^2\gamma, 6\gamma^4$
(20,12)	19	0.3614, 0.6385, 0.4577; 0.2401	$12\alpha^2\beta^2, 12\alpha^3\gamma^2$
(20,12)	29	0.3733, 0.8798, 0.1866; 0.2820	$12\alpha^3\beta, 12\alpha^2\beta\gamma^2$
(20,24)	25	0.3510, 0.5877, 0.4734; 0.1927	$24\alpha\beta^2\gamma, 12\alpha^3\gamma^2$
(44,12)	28	0.3590, 0.9229, 0.1024; 0.2301	$24\alpha^3\beta, 12\alpha^5\gamma^2$
(20,60)	23	0.3421, 0.6289, $\frac{2}{5}$; 0.1379	$60\alpha\beta^2\gamma, 12\gamma^5$
(16,6)	29	0.3861, 0.8415, 0.2805; 0.3188	$12\alpha^3\beta, 4\alpha^3\gamma^3$
(32,12)		0.3650, 0.9049, 0.1349; 0.2536	$24\alpha^3\beta, 6\alpha^4\gamma^4$
(80,30)		0.3480, 0.9558, 0.0519; 0.1766	$60\alpha^3\beta, 12\alpha^5\gamma^5$
(20,36)	24	0.3465, 0.6089, 0.4356; 0.1675	$36\alpha\beta^2\gamma, 12\alpha^2\gamma^3 : 2$
(32,6)	26	0.3686, 0.8939, 0.1566; 0.2665	$12\alpha^3\beta, 12\alpha^5\gamma : 5$
$(20 - 2m, m)$ $1 \leq m \leq 9$	7	$\frac{2}{5}, \frac{4}{5}, \frac{2}{5}; 0.3524$	$\alpha\beta^2, \beta^2\gamma, \alpha^3\beta,$ $\alpha^2\beta\gamma, \alpha\beta\gamma^2, \beta\gamma^3,$ $\alpha^5, \alpha^4\gamma, \alpha^3\gamma^2,$ $\alpha^2\gamma^3, \alpha\gamma^4, \gamma^5 : ?$
(20,24)	16	0.3579, 0.8210, 0.2315; 0.2257	$(12 + k)\alpha\beta^2, k\alpha^3\gamma^4,$ $(24 - 2k)\alpha^2\beta\gamma^2 : ?$ $0 \leq k < 12$

Table 1: 26 sporadic protosets.

The notation ? means the protoset admits a large number of different tilings, and we have not figured them out yet. The other 3D pictures are shown in Figure 4.

The numerical geometric data is listed in Table 1, where the angles and edge lengths are expressed in units of π , and the last column counts all vertices and also all tilings when they are not uniquely determined by the vertices. A rational fraction means the precise value. A decimal expression, such as $a = 0.4158$, means an approximate value $0.4158\pi < a < 0.4159\pi$. Moreover, the exact formulas are provided in the appendix.

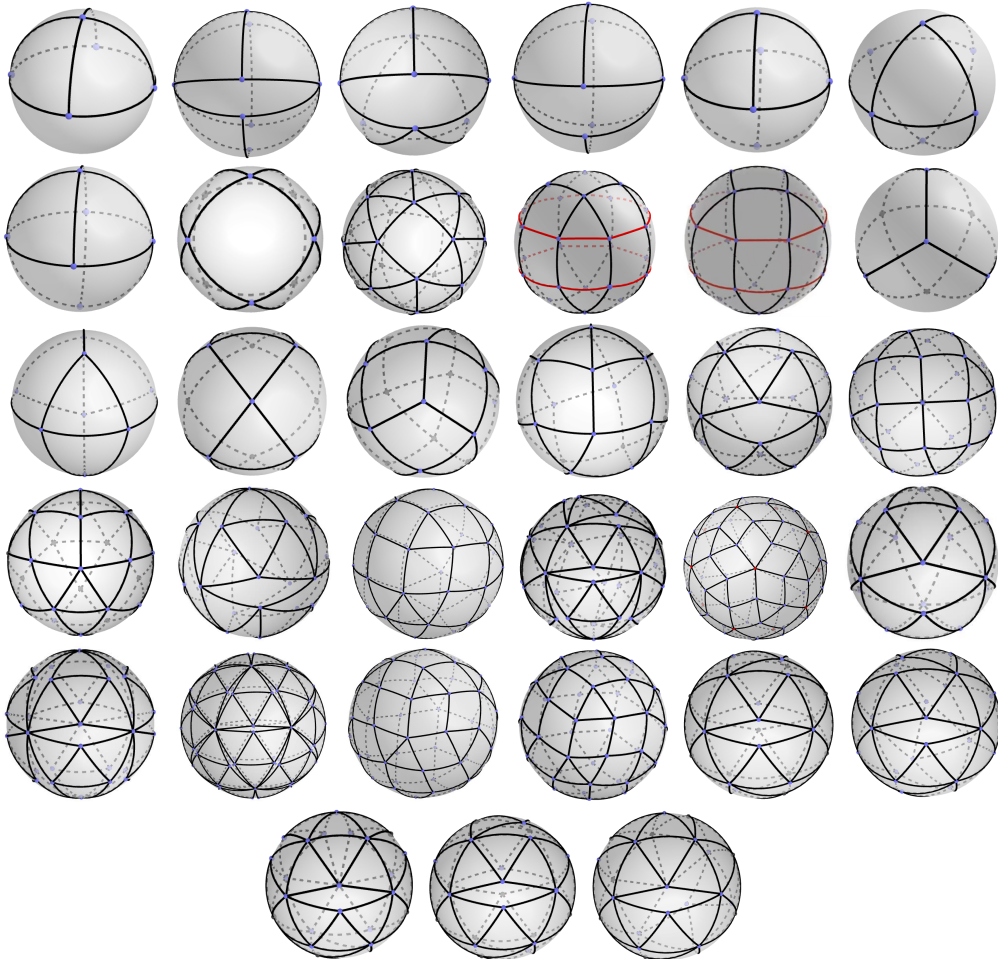


Figure 4: All 3D pictures in the fourth class except for two polymorphic ones.

Acknowledgement We would like to thank junior student Zhihong Lin for very helpful discussions in Case $\beta^2\gamma$. Thank two junior students Fangbin Chen and Nan Zhang for showing us how to draw Figure 3 and 4 using GeoGebra.

2 Basic Facts

Let v, e be the numbers of vertices and edges. Let v_k be the number of vertices of degree k . We have Euler's formula and basic counting equalities:

$$2 = v - e + f_{\Delta} + f_{\diamond},$$

$$2e = 3f_\Delta + 4f_\diamond = \sum_{k=3}^{\infty} kv_k = 3v_3 + 4v_4 + 5v_5 + \dots,$$

$$v = \sum_{k=3}^{\infty} v_k = v_3 + v_4 + v_5 + \dots.$$

Then it is easy to derive

$$v = 2 + \frac{1}{2}f_\Delta + f_\diamond, \quad (2.1)$$

$$3f_\Delta + 2f_\diamond = 12 + 2 \sum_{k=4}^{\infty} (k-3)v_k = 12 + 2v_4 + 4v_5 + 6v_6 + \dots, \quad (2.2)$$

$$v_3 + f_\Delta = 8 + \sum_{k=5}^{\infty} (k-4)v_k = 8 + v_5 + 2v_6 + \dots, \quad (2.3)$$

$$3v_3 + 2v_4 + v_5 = 12 + 2f_\diamond + \sum_{k=7}^{\infty} (k-6)v_k = 12 + 2f_\diamond + v_7 + 2v_8 + \dots. \quad (2.4)$$

We note that f_Δ is even and ≥ 2 by (2.1). The equality (2.2) show that $f_\Delta = 2, f_\diamond = 3$ for $v_k = 0 (k \geq 4)$, which is the simplest one. There must be some vertex of degree 3, 4 or 5 by (2.4).

We also have some geometric equations:

$$\begin{aligned} \cos a &= \cos^2 a + \sin^2 a \cos \alpha \\ &= \cot \alpha \cot \frac{\alpha}{2} \\ &= \cot \frac{\beta}{2} \cot \frac{\gamma}{2}. \end{aligned} \quad (2.5)$$

Then we deduce that

$$\left(\cot \frac{\beta}{2} \cot \frac{\gamma}{2}\right)^2 + [1 - \left(\cot \frac{\beta}{2} \cot \frac{\gamma}{2}\right)^2] \cos \alpha - \cot \frac{\beta}{2} \cot \frac{\gamma}{2} = 0, \quad (2.6)$$

$$\cot \frac{\beta}{2} \cot \frac{\gamma}{2} - \cot \alpha \cot \frac{\alpha}{2} = 0. \quad (2.7)$$

Lemma 1. *The simple application of the AAD:*

- There must be $|\alpha|\beta|\dots$ and $|\alpha|\gamma|\dots$ in an (a^3, a^4) -tiling.
- If $\beta^2 \dots$ or $|\beta|\beta|\dots$ is not a vertex, then $|\gamma|\gamma|\dots$ can never be a vertex.

Lemma 2. *In an (a^3, a^4) -tiling, we have $\frac{1}{3}\pi < \alpha < \pi, \beta > \frac{1}{2}\pi, \beta + \gamma > \pi$ and $0 < a < \frac{2}{3}\pi$.*

Proof. Since $3\alpha = \pi + S_\Delta$ and $2(\beta + \gamma) = 2\pi + S_\diamond$, we have $\alpha > \frac{1}{3}\pi$ and $\beta + \gamma > \pi$. By $\beta \geq \gamma$, we get $\beta > \frac{1}{2}\pi$.

If $\alpha \geq \pi$, then $S_\Delta \geq 2\pi$ and $f_\Delta S_\Delta \geq 4\pi$. This implies that $f_\diamond S_\diamond \leq 0$, a contradiction. So $\alpha < \pi$ i.e. $\frac{1}{3}\pi < \alpha < \pi$.

If $\alpha \rightarrow \pi$, then $S_\Delta \rightarrow 2\pi$, which imply the three vertices of the regular triangle are on the same equator and $a \rightarrow \frac{2}{3}\pi$. So $0 < a < \frac{2}{3}\pi$. \square

We will call an (a^3, a^4) -tiling or its protoset **convex** when $\beta < \pi$, **concave** when $\beta > \pi$, and **degenerate** when $\beta = \pi$.

Lemma 3. In any (a^3, a^4) -tiling, we have

- $0 < a < \frac{1}{2}\pi \iff \frac{1}{3}\pi < \alpha < \frac{1}{2}\pi < \beta < \pi$;
- $a = \frac{1}{2}\pi \iff \alpha = \frac{1}{2}\pi, \beta = \pi$;
- $\frac{1}{2}\pi < a < \frac{2}{3}\pi \iff \frac{1}{2}\pi < \alpha < \pi < \beta < 2\pi$.

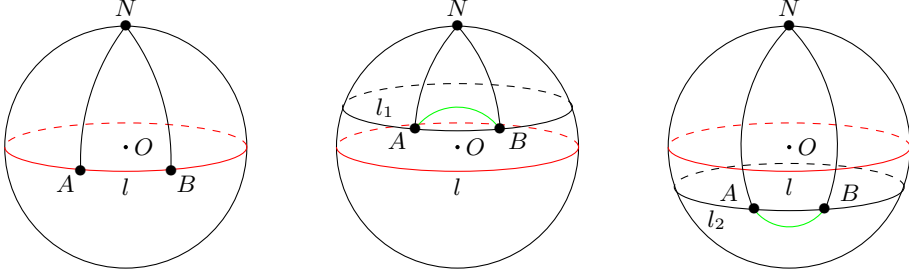


Figure 5: Proof of Lemma 3.

Proof. Let $\triangle NAB$ be the spherical isosceles triangle with $\widehat{NA} = \widehat{NB}$, N be the pole, O be the centre of sphere, l be the equator and l_1, l_2 be the latitude lines.

If $\widehat{NA} = \frac{1}{2}\pi$, then \widehat{AB} is on l and $\angle NAB = \frac{1}{2}\pi$. If $\widehat{NA} < \frac{1}{2}\pi$, then A, B are on l_1 and \widehat{AB} is above the l_1 . Since $\widehat{NA} \perp l_1$, we get $\angle NAB < \frac{1}{2}\pi$. Similarly if $\widehat{NA} > \frac{1}{2}\pi$, then $\angle NAB > \frac{1}{2}\pi$.

By considering the base angle, we have the same things happening for \widehat{NA} . Therefore we get this conclusion. \square

In fact, we see that $2\beta + 2\gamma - 2\pi < 4\gamma$ i.e. $\beta < \pi + \gamma$ in the third of Figure 5.

Lemma 4. In an (a^3, a^4) -tiling, α^3 can never be a vertex.

Proof. The vertex α^3 means $S_\Delta = \pi$ and $3 \leq f_\Delta \leq 4$. Since f_Δ is even, $f_\Delta = 4$ but $f_\Delta S_\Delta = 0$, a contradiction. Therefore, α^3 is not a vertex. \square

Lemma 5. In a convex (a^3, a^4) -tiling with $\gamma < \beta$, all vertices of degree 3, 4 or 5 are shown in Table 2.

degree	vertex
3	$\alpha\beta^2, \beta^3, \alpha\beta\gamma, \beta^2\gamma, \alpha\gamma^2, \beta\gamma^2, \gamma^3$
4	$\alpha^3\beta, \alpha^2\beta^2, \alpha\beta^3, \alpha^3\gamma, \alpha^2\beta\gamma, \alpha\beta^2\gamma, \alpha^2\gamma^2, \alpha\beta\gamma^2, \alpha\gamma^3, \beta\gamma^3, \gamma^4$
5	$\alpha^5, \alpha^4\beta, \alpha^4\gamma, \alpha^3\gamma^2, \alpha^2\beta\gamma^2, \alpha^2\gamma^3, \alpha\beta\gamma^3, \alpha\gamma^4, \beta\gamma^4, \gamma^5$

Table 2: Vertices of degree 3, 4, 5 for $\gamma < \beta < \pi$.

Proof. By Lemma 2 and 3, we have $\beta + \gamma > \pi$, $\frac{\pi}{3} < \alpha < \frac{\pi}{2} < \beta < \pi$, and $0 < \gamma < \beta$. If $\alpha^n\beta^m\gamma^l$ is a vertex, then we get $0 \leq n \leq 5, 0 \leq m \leq 3, l \geq 0, n + m + l \geq 3$.

By Lemma 4 and $2\alpha + \gamma < 2\alpha + \beta < 2\pi$, we know $\alpha^3, \alpha^2\beta$ or $\alpha^2\gamma$ can never be a vertex.

By $3\beta + \gamma > 2\beta + 2\gamma > 2\pi$ and $4\alpha < 2\pi$, we know $\beta^3\gamma, \beta^2\gamma^2$ or α^4 can never be a vertex.

When the degree is 5, we know $\beta^3 \cdots$ can never be a vertex by $3\beta + \gamma > 2\pi$ and $2\alpha + 3\beta > 2\pi$.

By $2\beta + 2\gamma > 2\pi$, $2\alpha + 2\beta + \gamma > 2\pi$ and $3\alpha + 2\beta > 2\pi$, we know $\beta^2 \cdots$ can never be a vertex.

By $3\alpha + \beta + \gamma > 2\pi$, we know $\alpha^3\beta\gamma$ can never be a vertex.

Therefore, we get all vertices of degree 3, 4 or 5 as listed in Table 2. \square

Lemma 6. In a convex (a^3, a^4) -tiling, if $\beta = \gamma$, then $\alpha < \beta < 2\alpha$.

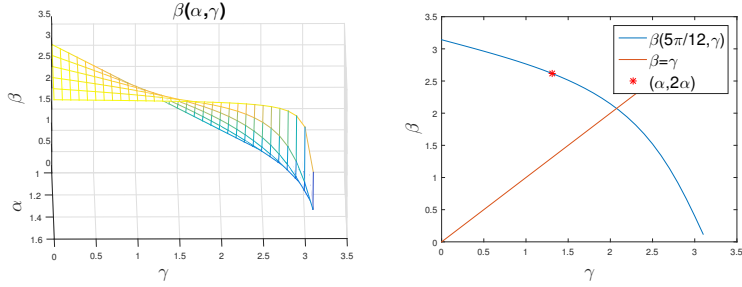


Figure 6: Proof of Lemma 6.

Proof. By Lemma 3, we have $0 < a < \frac{1}{2}\pi$, $\frac{1}{3}\pi < \alpha < \frac{1}{2}\pi$, and $0 < \gamma \leq \beta < \pi$. By (2.5), we get

$$\beta = 2\operatorname{arccot} \left(\cos a \tan \frac{\gamma}{2} \right) = 2\operatorname{arccot} \left(\cot \alpha \cot \frac{\alpha}{2} \tan \frac{\gamma}{2} \right).$$

If a or α is fixed, then we derive that

$$\beta' = -\frac{\cos a}{\cos^2 \frac{\gamma}{2} + (\cos a \sin \frac{\gamma}{2})^2} < 0.$$

So β is strictly decreasing with respect to γ (see the second of Figure 6). Moreover, there is a special case that two regular triangles can be merged into a rhombus *i.e.* $\beta = 2\alpha > \alpha = \gamma$. When $\beta = \gamma$, we have $\alpha < \gamma$ and $\beta < 2\alpha$ *i.e.* $\alpha < \beta < 2\alpha$. \square

Lemma 7. In a convex (a^3, a^4) -tiling, if $\beta = 2\alpha = 2\gamma$, then the tiling must be of the icosahedral type.

Proof. The $\beta = 2\alpha = 2\gamma$ means the rhombus is made of two regular triangles. So the (a^3, a^4) -tiling induces an a^3 -tiling. By Lemma 3, we have $\frac{1}{3}\pi < \alpha < \frac{1}{2}\pi$. Hence α^5 is the only vertex and we get the icosahedron. \square

Lemma 8. In a convex (a^3, a^4) -tiling, if $\gamma = \alpha$ or $\beta = k\gamma + (2 - k)\alpha$ for some constant $k \geq 0$, then the tiling must be of the icosahedral type.

Proof. When $\gamma = \alpha$, we get $\beta = 2\alpha$ by (2.7). In the proof of Lemma 6, we know $\beta = 2\operatorname{arccot} \left(\cos a \tan \frac{\gamma}{2} \right)$ is strictly decreasing with respect to γ for fixed a or α . When $k \geq 0$, $\beta = k\gamma + (2 - k)\alpha$ is increasing with respect to γ . So the two equations together have at most one solution. But $\gamma = \alpha, \beta = 2\alpha$ is an obvious solution to both equations. By Lemma 7, the convex (a^3, a^4) -tiling must be of the icosahedral type in either case. \square

We will call an (a^3, a^4) -tiling or its protoset **rational** when all angles (α, β, γ) are rational multiples of π .

Lemma 9. If the protoset is convex and rational, then the angles (α, β, γ) must be $(\frac{4}{9}, \frac{7}{9}, \frac{2}{3})\pi$, $(\frac{3}{7}, \frac{17}{21}, \frac{11}{21})\pi$ or $(\alpha, 2\alpha, \alpha)$ for any $\alpha \in (\mathbb{Q} \cap (\frac{1}{3}, \frac{1}{2}))\pi$.

Proof. By Lemma 3, we have $\frac{1}{3}\pi < \alpha < \frac{1}{2}\pi < \beta < \pi$, and $\beta \geq \gamma$, $\beta + \gamma > \pi$. Let $x = e^{i\alpha}, y = e^{i\beta}, z = e^{i\gamma}$. Then we derive $x^2y + x^2z - xyz - xy - xz - x + y + z = 0$ by (2.7).

Now we use the programs of [4, 7] in <https://github.com/kedlaya/tetrahedra/> to compute the cyclotomic points for this equation. It turns out that the only solutions within our range are the ones stated. \square

Proposition 10. Any convex rational (a^3, a^4) -tiling is either of the icosahedral type or $T(4a^3, 3a^4; 3\alpha^3\gamma, 3\alpha\beta^2, \gamma^3)$.

Proof. When $(\alpha, \beta, \gamma) = (\alpha, 2\alpha, \alpha)$, the (a^3, a^4) -tiling must be of the icosahedral type by Lemma 7. When $(\alpha, \beta, \gamma) = (\frac{3}{7}, \frac{17}{21}, \frac{11}{21})\pi$, $\alpha\gamma^3$ is the only vertex, contradicting Lemma 1.

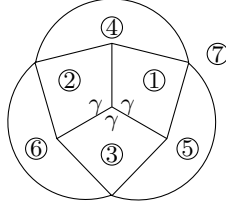


Figure 7: $T(4a^3, 3a^4; 3\alpha^3\gamma, 3\alpha\beta^2, \gamma^3)$.

When $(\alpha, \beta, \gamma) = (\frac{4}{9}, \frac{7}{9}, \frac{2}{3})\pi$, we have the AVC $\subset \{\alpha^3\gamma, \alpha\beta^2, \gamma^3\}$. The AAD $|\gamma^\beta|^\alpha|\alpha| \cdots$ of $\alpha^3\gamma$ gives $|\alpha|^\beta|\alpha| \cdots = \alpha\beta^2$ and the AAD $|\beta^\gamma|^\alpha|\alpha| \cdots$ of $\alpha\beta^2$ gives $|\gamma|^\beta|\alpha| \cdots = \gamma^3$. So γ^3 must appear, which determines T_1, T_2, T_3 in Figure 7. Then $\beta^2 \cdots = \alpha\beta^2$ determines T_4, T_5, T_6 ; $\alpha^2\gamma \cdots = \alpha^3\gamma$ determines T_7 . The tiling is completed and the 3D picture is the 12th of Figure 4. \square

A vertex $\alpha^{n_1}\beta^{n_2}\gamma^{n_3}$ can be efficiently represented by its vector type $\mathbf{n} = (n_1 \ n_2 \ n_3) \in \mathbb{N}^3$. We will use both representations interchangeably afterwards for convenience.

Lemma 11 (Irrational Angle Lemma). *Given two different vertices $\mathbf{l}, \mathbf{m} \in \mathbb{N}^3$ in an (a^3, a^4) -tiling with some irrational angle, if there is another vertex \mathbf{n} , then $\mathbf{l}, \mathbf{m}, \mathbf{n}$ are linearly dependent. In other words, the square matrix of $\mathbf{l}, \mathbf{m}, \mathbf{n}$ has determinant 0.*

Proof. By the vertices $\mathbf{l}, \mathbf{m}, \mathbf{n}$, the angles satisfy a linear system of equations

$$\begin{pmatrix} \mathbf{l} \\ \mathbf{m} \\ \mathbf{n} \end{pmatrix} \begin{pmatrix} \alpha \\ \beta \\ \gamma \end{pmatrix} = \begin{pmatrix} 2 \\ 2 \\ 2 \end{pmatrix} \pi.$$

If $\mathbf{l}, \mathbf{m}, \mathbf{n}$ are linearly independent, then the system has a unique rational solution, a contradiction. \square

In Section 4 and 5, we will use Lemma 11 to handle the convex (a^3, a^4) -tiling with some irrational angle, which imposes strong constraints on all possible vertices. But before that, we will discuss the short and easier concave and degenerate cases first in the next section.

3 Concave and degenerate cases $\beta \geq \pi$

Since all vertices have degree ≥ 3 , $\beta^2 \cdots$ is not a vertex. By Lemma 1, $|\gamma|^\beta|\alpha| \cdots$ can never be a vertex and $|\alpha|^\beta|\alpha| \cdots$ must appear.

$\beta > \pi$

By Lemma 3, we have $\frac{1}{2}\pi < \alpha < \pi$ and $|\alpha|^\beta|\alpha| \cdots = \alpha\beta\gamma$, which determines T_1, T_2, T_3 in Figure 8. Then $|\beta_3|^\beta|\alpha| \cdots = |\beta_3|^\beta|\alpha|$ determines T_4 , $|\alpha_1|^\beta|\alpha| \cdots = \alpha\beta\gamma$ determines T_5 and we get a tiling like a triangular prism.

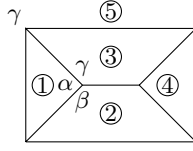


Figure 8: $T(2a^3, 3a^4; 6\alpha\beta\gamma)$.

$\beta = \pi$

By Lemma 3, we have $\alpha = \frac{1}{2}\pi$ and $|\alpha|\beta|\dots = \alpha^2\beta, \alpha\beta\gamma$.

Case $\alpha\beta\gamma$

We have $\gamma = \frac{1}{2}\pi$. In Figure 9, $\alpha\beta\gamma$ determines T_1, T_2, T_3 ; $|\beta|\gamma|\dots = |\beta|\gamma|\alpha|$ determines T_4 . When one of $|\alpha_1|\beta_3|\dots$ and $|\alpha_4|\beta_2|\dots$ is $\alpha\beta\gamma$, the tiling is the same as Figure 8. When they are $\alpha^2\beta$, T_5, T_6 are determined and the 3D picture is the 6th of Figure 4.

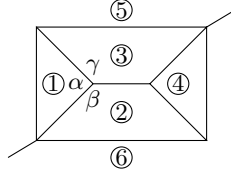


Figure 9: $T(4a^3, 2a^4; 2\alpha\beta\gamma, 2\alpha^2\beta, 2\alpha^3\gamma)$.

Case $\alpha^2\beta$

By $\alpha^2\beta = |\beta\gamma|\alpha|\alpha|$ and similar proof of Lemma 5, we get $|\alpha|\gamma|\dots = \alpha\beta\gamma^2, \alpha^2\gamma, \alpha^2\gamma^2, \alpha^3\gamma, \alpha^3\gamma^2, \alpha^3\gamma^3$, and $|\alpha|\beta|\dots$ can only be $\alpha^2\beta$.

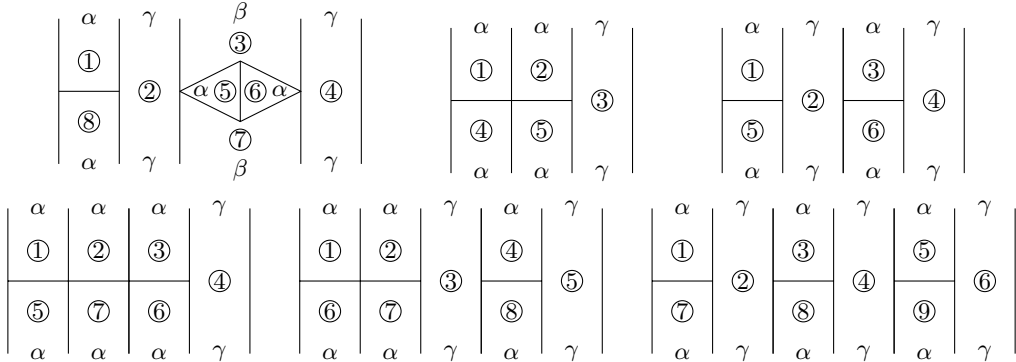


Figure 10: $|\alpha|\gamma|\dots = \alpha\beta\gamma^2, \alpha^2\gamma, \alpha^2\gamma^2, \alpha^3\gamma, \alpha^3\gamma^2, \alpha^3\gamma^3$.

When $|\alpha|\gamma|\dots = \alpha\beta\gamma^2$, we have $\gamma = \frac{1}{4}\pi$. The vertex $\alpha\beta\gamma^2 = |\alpha|\gamma|\beta|\gamma|$ determines T_1, \dots, T_4 in the first of Figure 10; $|\beta|\gamma|\dots = |\beta|\gamma|\alpha|\dots = |\beta|\gamma|\alpha|\gamma|$ determines T_5, T_6, T_7 ; $|\alpha|\beta|\dots = \alpha^2\beta$ determines T_8 .

We omit the details and claim that the other possibilities of $|\alpha|\gamma|\dots$ produce exactly the other tilings in Figure 10. The 3D pictures are the 3rd, 1st, 5th, 7th, 4th and 2nd of Figure 4, respectively.

4 Convex case $\gamma = \beta < \pi$ with some irrational angle

By Lemma 3 and 6, we have $\frac{\pi}{3} < \alpha < \frac{\pi}{2} < \beta < 2\alpha$. By Lemma 1 and similar proof of Lemma 5, we get $|\alpha|\beta|\dots = \alpha\beta^2, \alpha\beta^3, \alpha^2\beta^2, \alpha^3\beta, \alpha^4\beta$. The Lemma 11 implies that there is only one kind of vertex in all such tilings.

Case $|\alpha|\beta|\dots = \alpha\beta^2$, $\text{AVC} \subset \{\alpha\beta^2\}$

By the AVC, we can get a tiling which is the same as Figure 8.

Case $|\alpha|\beta|\dots = \alpha\beta^3$, $\text{AVC} \subset \{\alpha\beta^3\}$

The vertex $\alpha\beta^3$ determines T_1, T_2, T_3, T_4 in Figure 11; $\alpha\beta\dots = \alpha\beta^3$ determines T_5, T_6, T_7 . Since the symmetry of the partial tiling and $\beta^2\dots = \alpha\beta^3$, we have four cases:

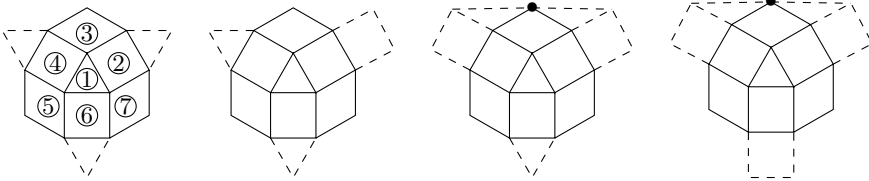


Figure 11: $\alpha\beta^3$ is the vertex.

In the third and fourth cases, we get $\alpha^2\beta\dots$, contradicting the AVC. In the first case, we can determine T_8, T_9, \dots, T_{26} as the first of Figure 12 and its 3D picture is the 10th of Figure 4 corresponding to the rhombicuboctahedron. In the second case, we get a different tiling as the second of Figure 12 and its 3D picture is the 11th of Figure 4 corresponding to the elongated square gyrobicupola. By rotating the partial tiling with the red boundary 45° , the first tiling will become the second.

Case $|\alpha|\beta|\dots = \alpha^2\beta^2$, $\text{AVC} \subset \{\alpha^2\beta^2\}$

The vertex $\alpha^2\beta^2$ is $|\alpha|\alpha|\beta|\beta|$ or $|\alpha|\beta|\alpha|\beta|$. In the third of Figure 12, $|\alpha|\alpha|\beta|\beta|$ determines T_1, T_2, T_3, T_4 ; $\beta^2\dots = \alpha^2\beta^2$ determines T_5, T_6 ; $\alpha^2\dots = \alpha^2\beta^2$ determines T_7, \dots, T_{10} . Similarly, $T_{11}, T_{12}, T_{13}, T_{14}$ are determined and its 3D picture is a triangular orthobicupola. Next $\alpha^2\beta^2$ can only be $|\alpha|\beta|\alpha|\beta|$. Then we get a new tiling in the fourth of Figure 12 and its 3D picture is a cuboctahedron. By rotating the partial tiling with the red boundary 60° or flipping the partial tiling with the red boundary, the first tiling will become the second.

Case $|\alpha|\beta|\dots = \alpha^3\beta$, $\text{AVC} \subset \{\alpha^3\beta\}$

By the AVC, we can get a tiling in the fifth of Figure 12 and its 3D picture is the 8th of Figure 4 corresponding to one of the anti-prisms.

Case $|\alpha|\beta|\dots = \alpha^4\beta$, $\text{AVC} \subset \{\alpha^4\beta\}$

In the sixth of Figure 12, $\alpha^4\beta$ determines T_1, \dots, T_5 , $\alpha\beta\dots = \alpha^4\beta$ determines T_6, \dots, T_{13} . Since the symmetry of the partial tiling and $\alpha^3\dots = \alpha^4\beta$, we might as well take $|\alpha_3|\alpha_4|\alpha_6|\alpha|\beta|\dots = |\alpha_3|\alpha_4|\alpha_6|\alpha|\beta|$ which determines T_{14}, T_{15} . Then we can determine T_{16}, \dots, T_{38} and its 3D picture is the 9th of Figure 4 corresponding to a snub cube.

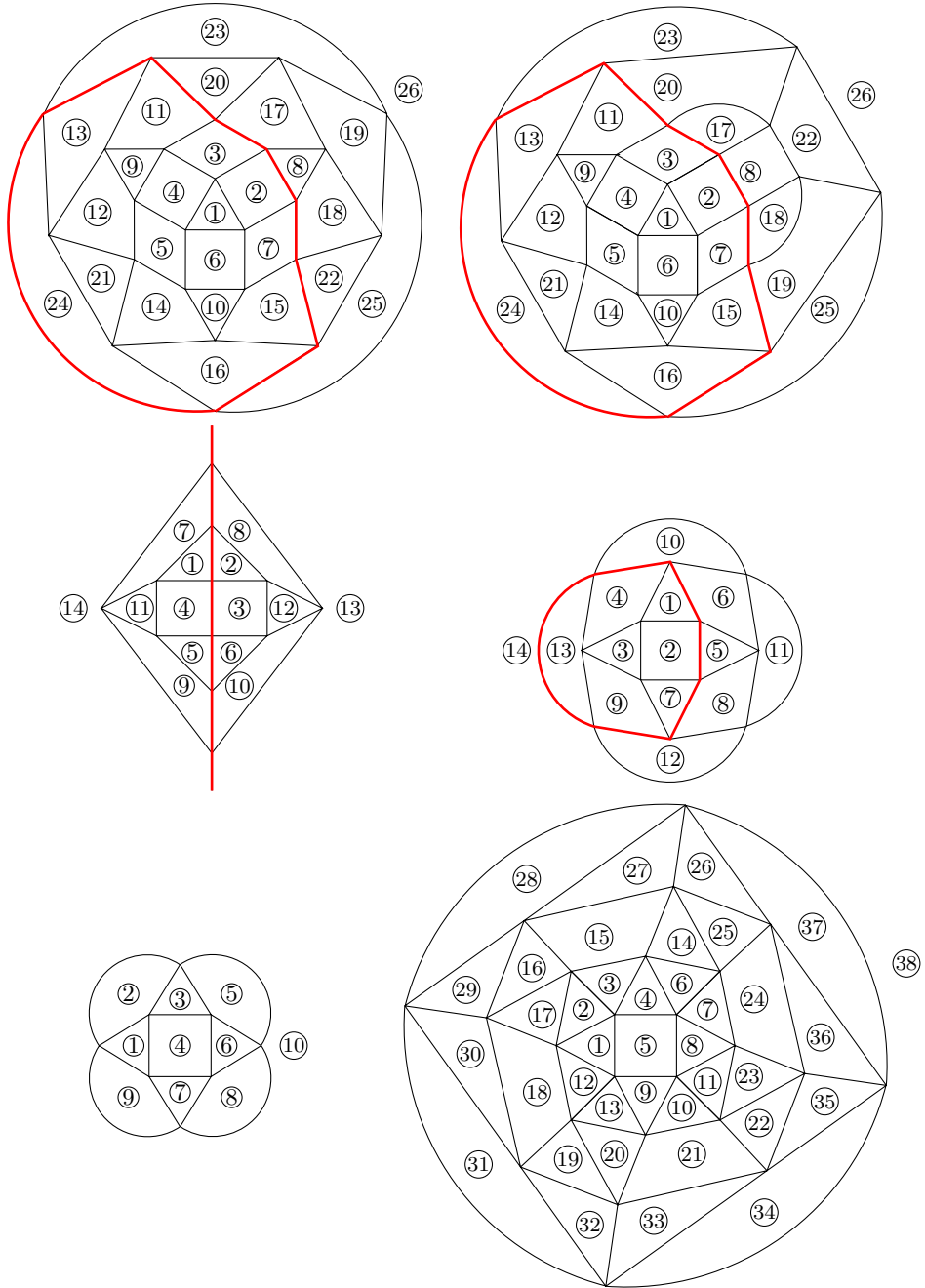


Figure 12: $|\alpha|\beta|\dots = \alpha\beta^3, \alpha^2\beta^2, \alpha^3\beta, \alpha^4\beta$.

5 Convex case $\gamma < \beta < \pi$ with some irrational angle

By Lemma 2 and 3, we have $\beta + \gamma > \pi$, $\frac{\pi}{3} < \alpha < \frac{\pi}{2} < \beta < \pi$, and $0 < \gamma < \beta$. By Lemma 5, we only need to discuss the vertices in Table 2 case by case. In each case, we can get the AVC by Lemma 11.

5.1 The vertex types of degree 3

Case $\alpha\gamma^2$

The AAD $|\alpha\gamma^\beta|\beta\gamma|$ of $\alpha\gamma^2$ gives $|\beta|\beta|\dots$. Similar to the proof of Lemma 5, $\beta^2\dots$ can never be a vertex.

Case $\beta\gamma^2$

By $3\beta > \beta + 2\gamma = 2\pi$, we have $\pi > \beta > \frac{2\pi}{3}$, $\alpha < \frac{\pi}{2} < \gamma < \frac{2\pi}{3} < 2\alpha$. The vertex $\beta\gamma^2$ determines T_1, T_2, T_3 in the left of Figure 13; $\beta^2\dots = \alpha\beta^2$ determines T_4 ; $\beta\gamma\dots = \beta\gamma^2$ determines T_5 . But $\alpha\beta\gamma\dots$ appears, contradicting $\beta\gamma\dots = \beta\gamma^2$.

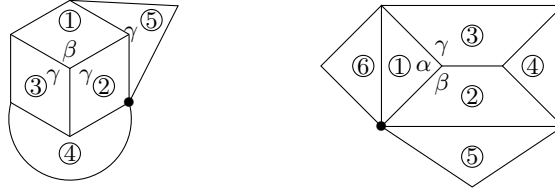


Figure 13: $\beta\gamma^2$ or $\alpha\beta\gamma$ is a vertex.

Case $\alpha\beta\gamma$

Similar to the proof of Lemma 5, $\beta^2\dots$ can never be a vertex. So $|\gamma|\gamma|\dots$ can never be a vertex by Lemma 1. In the right of Figure 13, $\alpha\beta\gamma$ determines T_1, T_2, T_3 , $|\beta|\gamma|\dots = |\beta|\gamma|\alpha|$ determines T_4 , and we get $\alpha\beta\dots = \alpha\beta\gamma, \alpha^2\beta, \alpha^3\beta$.

When one of $|\alpha_1|\beta_3|\dots$ and $|\alpha_4|\beta_2|\dots$ is $\alpha\beta\gamma$, the tiling is the same as Figure 8. When one of them is $\alpha^2\beta$, we get $\gamma = \alpha$. Then we conclude that either there is no tilings or there is tilings which must be of the icosahedral type by Lemma 8. In a similar discussion later, we will omit the details. When they are $\alpha^3\beta$, T_5, T_6 are determined and we get $\gamma = 2\alpha$. But $\alpha^3\gamma\dots$ can never be a vertex.

Case β^3

We have $\beta = \frac{2}{3}\pi, \gamma > \frac{1}{3}\pi$. By $\beta^3 = |\beta\gamma|\gamma\beta|\beta|$ and similar proof of Lemma 5, we get $|\gamma|\gamma|\dots = \alpha\beta\gamma^2, \beta\gamma^3, \alpha^3\gamma^2, \alpha^2\gamma^2, \alpha^2\gamma^3, \alpha\gamma^3, \alpha\gamma^4, \gamma^4, \gamma^5$.

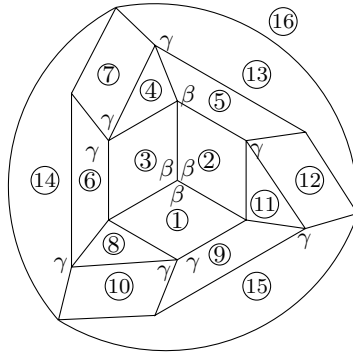


Figure 14: $T(4\alpha^3, 12\alpha^4; 12\alpha\beta\gamma^2, 4\beta^3)$.

When $|\gamma|\gamma|\dots = \alpha\beta\gamma^2$, we get the AVC $\subset \{\beta^3, \alpha\beta\gamma^2\}$ by Lemma 11. The vertex β^3 determines T_1, T_2, T_3 in Figure 14. By the symmetry of the partial tiling and $\gamma^2 \dots = \alpha\beta\gamma^2$, we might as well take $|\gamma_2|\gamma_3|\dots = |\gamma_2|\gamma_3|\alpha|\beta|$ which determines T_4, T_5 ; $\alpha\beta \dots = \alpha\beta\gamma^2$ determines T_6, T_7 . Similarly, T_8, T_9, \dots, T_{16} are determined and the 3D picture is the 15th of Figure 4.

$ \gamma \gamma \dots$	AVC \subset a set	Conclusion
$\beta\gamma^3$	$\{\beta^3, \beta\gamma^3\}$	No $\alpha\beta \dots$, contradicting Lemma 1
$\alpha^3\gamma^2$	$\{\beta^3, \alpha^3\gamma^2\}$	
$\alpha^2\gamma^k, k = 2, 3$	$\{\beta^3, \alpha^2\gamma^k\}$	
$\alpha\gamma^k, k = 3, 4$	$\{\beta^3, \alpha\gamma^k\}$	
$\gamma^k, k = 4, 5$	$\{\beta^3, \gamma^k\}$	

Table 3: The simple cases when β^3 appears.

Case $\beta^2\gamma$

By $\beta^2\gamma = |\gamma^\beta|\gamma|\beta|\beta|$ and similar proof of Lemma 5, we get $|\beta|\gamma|\dots = \beta^2\gamma, \alpha\beta\gamma^h (h \geq 3), \alpha^2\beta\gamma^j (j \geq 2), \beta\gamma^k (k \geq 4)$.

Subcase $|\beta|\gamma|\dots = \beta\gamma^k (k \geq 4)$, AVC $\subset \{\beta^2\gamma, \beta\gamma^k, \gamma^{2k-1}\}$

There is no the vertex $\alpha\beta \dots$, contradicting Lemma 1.

Subcase $|\beta|\gamma|\dots = \alpha\beta\gamma^h (h \geq 3)$, AVC $\subset \{\beta^2\gamma, \alpha\beta\gamma^h, \alpha^2\gamma^{2h-1}\}$

When $|\gamma|\alpha|\gamma|\dots$ appears, T_1, T_2, T_3 are determined in Figure 15. Then one of $|\alpha_1|\beta_2|\dots$ and $|\alpha_1|\beta_3|\dots$ must be $\alpha\beta^2 \dots$, contradicting the AVC. So $\alpha\beta\gamma^h = |\alpha|\beta|\gamma|\dots|\gamma|$.

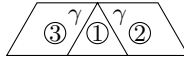


Figure 15: $|\gamma|\alpha|\gamma|\dots$ appears.

If $h = 3$, then $|\alpha|\beta|\gamma|\gamma|\gamma|$ determines T_1, \dots, T_5 in Figure 16; $\alpha\beta \dots = \alpha\beta\gamma^3$ determines T_6, \dots, T_{10} ; $\beta^2 \dots = \beta^2\gamma$ determines T_{11}, \dots, T_{16} ; $\beta\gamma^3 \dots = \alpha\beta\gamma^3$ determines T_{17} . The 3D picture is the 4th of Figure 3. If $h > 3$, then we have the same tilings $T(2a^3, xa^4; 6\alpha\beta\gamma^h, y\beta^2\gamma)$. By $y + 3 = x$ and $3h + \frac{y}{2} = x$, we get $x = 6h - 3, y = 6h - 6$.

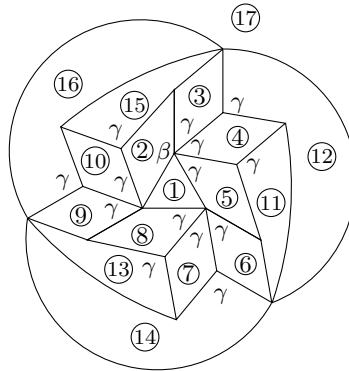


Figure 16: $T(2a^3, 15a^4; 6\alpha\beta\gamma^3, 12\beta^2\gamma)$.

By $\gamma = 2\pi - 2\beta, \alpha = (1 - h)2\pi + (2h - 1)\beta$ and (2.6), we obtain $2 \cos \alpha \cos \beta - \cos \beta - \cos \alpha = \cos \alpha(2 \cos \beta - 1) - \cos \beta = 0$. Let $f(h, \beta) = \cos \alpha(2 \cos \beta - 1) - \cos \beta$, we have $f'_\beta = -(2h - 1) \sin \alpha(2 \cos \beta - 1) + \sin \beta(1 - 2 \cos \alpha)$.

Since $\alpha \in (\frac{\pi}{3}, \frac{\pi}{2})$, we get $\beta \in (\beta_{min}, \beta_{max})$, where $\beta_{min} = \frac{\frac{\pi}{3} + (h-1)2\pi}{2h-1} = \pi - \frac{\frac{2}{3}\pi}{2h-1} > \frac{2}{3}\pi, \beta_{max} = \frac{\frac{\pi}{2} + (h-1)2\pi}{2h-1} = \pi - \frac{\frac{\pi}{2}}{2h-1} < \pi$. Obviously, $f'_\beta > 0, f(h, \beta_{min}) < 0, f(h, \beta_{max}) > 0$. This implies that $\forall h \geq 3, f(h, \beta) = 0$ has a unique solution in $(\beta_{min}, \beta_{max})$. Moreover,

$$\frac{d\beta}{dh} = -\frac{f'_h}{f'_\beta} = -\frac{-(2 \cos \beta - 1) \sin \alpha(2\beta - 2\pi)}{f'_\beta} > 0.$$

This means β is monotonically increasing with respect to h .

By $\lim_{h \rightarrow +\infty} \beta_{min} = \lim_{h \rightarrow +\infty} \beta_{max} = \pi$, we get $\lim_{h \rightarrow +\infty} \beta = \pi, \lim_{h \rightarrow +\infty} \gamma = 0$. We observe that there are three a -edges between the poles, so $\lim_{h \rightarrow +\infty} a = \frac{\pi}{3}$ and $\lim_{h \rightarrow +\infty} \alpha = \arccos \frac{1}{3}$.

Subcase $|\beta|\gamma|\dots = \alpha^2\beta\gamma^j (j \geq 2), AVC \subset \{\beta^2\gamma, \alpha^2\beta\gamma^j, \alpha^4\gamma^{2j-1}\}$

As shown in figure 15, when $|\gamma|\alpha|\gamma|\dots$ appears, we get two $|\alpha|\beta|\dots = |\gamma|\alpha|\alpha|\beta|\dots$. But $\alpha\beta^2 \dots$ appears, contradicting the AVC. So $|\beta|\gamma|\dots = \alpha^2\beta\gamma^j = |\alpha|\alpha|\gamma|\dots$ determines T_1, T_2, T_3 in Figure 17. Then $|\beta_3|\alpha_2|\dots$ is either $|\beta_3|\alpha_2|\alpha|\dots$ or $|\beta_3|\alpha_2|\gamma|\dots$.

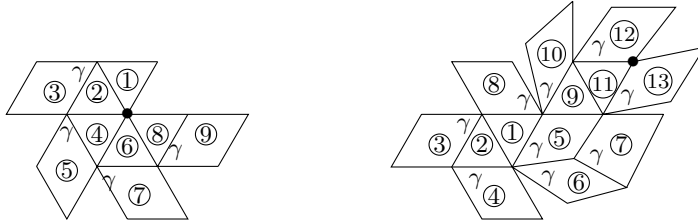


Figure 17: $|\alpha|\alpha|\gamma|\dots$ appears.

When $|\beta_3|\alpha_2|\alpha|\dots$ appears, $|\beta_3|\alpha_2|\alpha|\dots = |\beta_3|\alpha_2|\alpha|\gamma|\dots$ determines T_4, T_5 in the first; $|\beta_5|\alpha_4|\dots = |\beta_5|\alpha_4|\alpha|\gamma|\dots$ determines T_6, T_7 . Similarly, T_8, T_9 are determined but $\alpha^5 \dots$ appears, contradicting the AVC.

When $|\beta_3|\alpha_2|\gamma|\dots$ appears, T_4 is determined in the second. Then $|\beta_4|\alpha_2|\alpha_1|\dots = \alpha^2\beta\gamma^j$ determines T_5, T_6 ; $\beta^2 \dots = \beta^2\gamma$ determines T_7 . Since $|\alpha_2|\alpha_1|\gamma_5|\dots$ appears, $|\beta_5|\alpha_1|\dots = |\beta_5|\alpha_1|\gamma|\dots = |\gamma|\alpha|\beta_5|\alpha_1|\gamma|\dots$ determines T_8, T_9, T_{10} . Similarly, we can determine T_{11}, T_{12}, T_{13} but $\alpha\beta^2 \dots$ appears, contradicting the AVC.

Subcase $|\beta|\gamma|\dots$ can only be $\beta^2\gamma$

Then we have the monohedral tiling in Figure 18, a contradiction.

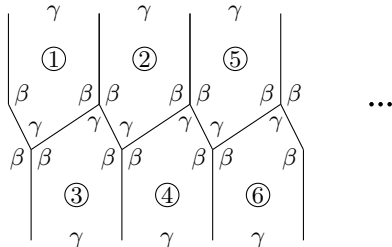


Figure 18: $T(f_\diamond \beta^2\gamma, 2\gamma^{f_\diamond/2})$.

Case $\alpha\beta^2$

By $2\beta + 2\gamma > 2\pi = \alpha + 2\beta$, we have $2\gamma > \alpha > \frac{1}{3}\pi$ i.e. $\gamma > \frac{1}{6}\pi$. The AAD $|\alpha|\beta^\gamma|\gamma\beta|$ of $\alpha\beta^2$ gives $|\gamma|\gamma|\dots$. Similar to the proof of Lemma 5, all possibilities of $|\gamma|\gamma|\dots$ are listed in Table 4.

$\beta\gamma^4, \beta\gamma^5, \beta\gamma^6, \alpha\beta\gamma^3, \alpha\beta\gamma^4, \alpha^2\beta\gamma^2$
$\gamma^3, \gamma^4, \gamma^6, \gamma^7, \gamma^8, \gamma^9, \gamma^{10}, \gamma^{11}$
$\alpha\gamma^3, \alpha\gamma^5, \alpha\gamma^6, \alpha\gamma^7, \alpha\gamma^8, \alpha\gamma^9$
$\alpha^2\gamma^2, \alpha^2\gamma^4, \alpha^2\gamma^5, \alpha^2\gamma^6, \alpha^2\gamma^7$
$\alpha^3\gamma^3, \alpha^3\gamma^4, \alpha^3\gamma^5$
$\alpha^4\gamma^2, \alpha^4\gamma^3$

Table 4: All possibilities of $|\gamma|\gamma|\dots$.

$ \gamma \gamma \dots$	AVC \subset a set	Conclusion
$\beta\gamma^k, k = 4, 5, 6$	$\{\alpha\beta^2, \beta\gamma^k\}$	No $\alpha\gamma\dots$, contradicting Lemma 1
$\gamma^k, k = 3, 4, 6, \dots, 11$	$\{\alpha\beta^2, \gamma^k\}$	

Table 5: The simple cases when $\alpha\beta^2$ appears.

Subcase $|\gamma|\gamma|\dots = \alpha\beta\gamma^k (k = 3, 4)$, $\text{AVC} \subset \{\alpha\beta^2, \alpha\beta\gamma^k, \alpha\gamma^{2k}\}$

As shown in Figure 15, when $|\gamma|\alpha|\gamma|\dots$ appears, we get two $|\alpha|\beta|\dots$ and one of them must be $|\alpha|\beta|\gamma|\dots|\gamma|$. Since $|\gamma|\gamma|\dots$ is either $|\gamma|\alpha|\gamma|\dots$ or $|\alpha|\beta|\gamma|\dots|\gamma|$, there must be $|\gamma|\gamma|\gamma|\dots$ which determines T_1, T_2, T_3 in Figure 19. Then $\beta^2\dots = \alpha\beta^2$ determines T_4, T_5 . But $\alpha^2\gamma\dots$ appears, contradicting the AVC.

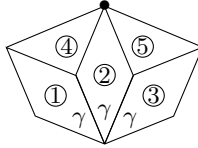


Figure 19: $|\gamma|\gamma|\gamma|\dots$ appears.

Subcase $|\gamma|\gamma|\dots = \alpha^2\beta\gamma^2$, $\text{AVC} \subset \{\alpha\beta^2, \alpha^2\beta\gamma^2, \alpha^3\gamma^4\}$

Similarly, when $|\gamma|\alpha|\gamma|\dots$ appears, one of the two $|\alpha|\beta|\dots$ must be $\alpha^2\beta\gamma^2$. Moreover, the vertex $\alpha^3\gamma^4$ has four arrangements in Figure 20. In the first, if $|\alpha_{10}|\gamma_5|\alpha_9|\dots = |\alpha_{10}|\gamma_5|\alpha_9|\gamma|\dots$, then $\alpha^2\beta\gamma^2$ appears; if $|\alpha_{10}|\gamma_5|\alpha_9|\dots = |\alpha_{10}|\gamma_5|\alpha_9|\beta|\dots$, then it is $\alpha^2\beta\gamma^2$; if $|\alpha_{10}|\gamma_5|\alpha_9|\dots = |\alpha_{10}|\gamma_5|\alpha_9|\alpha|\dots = |\gamma|\alpha_{10}|\gamma_5|\alpha_9|\alpha|\gamma|\dots$, then $\alpha^2\beta\gamma^2$ appears. Since the others have $|\gamma|\alpha|\gamma|\dots$, there must be the vertex $\alpha^2\beta\gamma^2$.

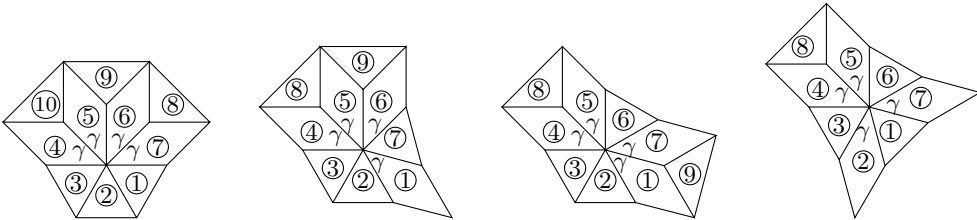


Figure 20: The vertex arrangements for $\alpha^3\gamma^4$.

Without $\alpha^3\gamma^4$, we have the tiling $T(20a^3, 24a^4; 12\alpha\beta^2, 24\alpha^2\beta\gamma^2)$ with 24 different tilings in Figure 21.

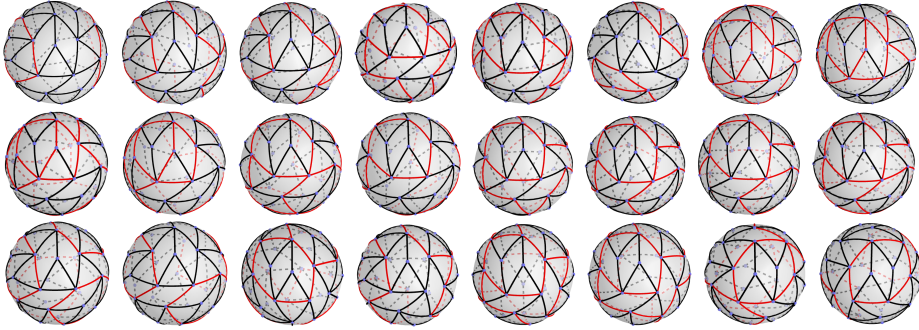


Figure 21: $T(20a^3, 24a^4; 12\alpha\beta^2, 24\alpha^2\beta\gamma^2)$.

In these tilings, we find a module in Figure 22. The flip of the module with respect to line L keeps the angle sums of all vertices and transforms the tiling to a new tiling $T(20a^3, 24a^4; (12 + k)\alpha\beta^2, (24 - 2k)\alpha^2\beta\gamma^2, k\alpha^3\gamma^4)$, where $0 \leq k \leq 11$. For example, A, B are vertices of degree 5, by flipping, A become a vertex of degree 7 and B become a vertex of degree 3. This indicates that for every vertex of degree 7 added, one vertex of degree 3 will be added and two vertices of degree 5 will be reduced.

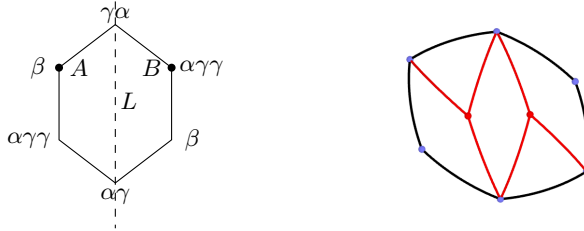


Figure 22: The basic module.

Since the diversity of the number, arrangement and position of $\alpha^3\gamma^4$ and $\alpha^2\beta\gamma^2$, the complexity of the tilings is greatly increased.

Subcase $|\gamma|\gamma|\dots = \alpha\gamma^k (k = 3, 5, 7, 9)$, $AVC \subset \{\alpha\beta^2, \alpha\gamma^k\}$

There must be $|\gamma|\gamma|\gamma|\dots$. As shown in figure 19, we get $\alpha^2\gamma\dots$, contradicting the AVC.

Subcase $|\gamma|\gamma|\dots = \alpha^2\gamma^2$, $AVC \subset \{\alpha\beta^2, \alpha^2\gamma^2\}$

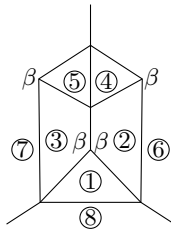


Figure 23: $T(4a^3, 4a^4; 4\alpha\beta^2, 4\alpha^2\gamma^2)$.

In Figure 23, $\alpha\beta^2$ determines T_1, T_2, T_3 ; $\gamma^2 \dots = \alpha^2\gamma^2$ determines T_4, T_5 ; $\alpha^2 \dots = \alpha^2\gamma^2$ determines T_6, T_7 ; $\alpha\gamma^2 \dots = \alpha^2\gamma^2$ determines T_8 . The 3D picture is the 13th of Figure 4.

Subcase $|\gamma|\gamma|\dots = \alpha^2\gamma^k (k = 4, \dots, 7)$, $\text{AVC} \subset \{\alpha\beta^2, \alpha^2\gamma^k\}$

When $|\gamma|\alpha|\gamma|\dots$ appears, one of the two $|\alpha|\beta|\dots$ must be $|\gamma|\alpha|\beta|\dots$, contradicting the AVC. So $\alpha^2\gamma^k = |\alpha|\alpha|\gamma|\dots|\gamma|$. As shown in figure 19, $|\alpha|\gamma|\alpha|\dots$ appears, a contradiction. Then $|\gamma|\gamma|\dots = \alpha^3\gamma^k (k = 3, 5)$ is also impossible.

Subcase $|\gamma|\gamma|\dots = \alpha^4\gamma^k (k = 2, 3)$, $\text{AVC} \subset \{\alpha\beta^2, \alpha^4\gamma^k\}$

Similarly, $|\gamma|\alpha|\gamma|\dots$ is not a vertex. When $k = 2$, $\alpha\beta^2$ determines T_1, T_2, T_3 as the first of Figure 24; $\gamma^2 \dots = \alpha^4\gamma^2$ determines T_4, \dots, T_7 ; $\alpha^2 \dots = \alpha^4\gamma^2$ determines T_8, T_9, T_{10}, T_{11} ; $\alpha\beta \dots = \alpha\beta^2$ determines T_{12}, T_{13} . But $|\gamma_{12}|\alpha_4|\alpha_5|\alpha_8|\gamma_{13}|\dots = |\gamma_{12}|\alpha_4|\alpha_5|\alpha_8|\gamma_{13}|\alpha|$, a contradiction.

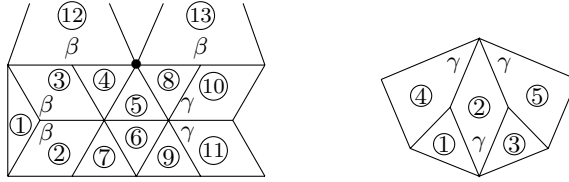


Figure 24: $|\gamma|\gamma|\dots = \alpha^4\gamma^k (k = 2, 3)$.

When $k = 3$, we get $|\gamma|\gamma|\dots = |\alpha|\alpha|\alpha|\alpha|\gamma|\gamma|\gamma|$, $|\gamma|\gamma|\alpha|\alpha|\alpha|\alpha|$. The latter determines T_1, T_2, T_3 as the second of Figure 24; $\alpha\beta \dots = \alpha\beta^2$ determines T_4, T_5 . Then $|\gamma_4|\gamma_2|\gamma_5|\dots = |\alpha|\alpha|\alpha|\alpha|\gamma_4|\gamma_2|\gamma_5|$ and $|\alpha|\alpha|\alpha|\alpha|\gamma|\gamma|\gamma|$ must appear. Similar to the first of Figure 24, $|\gamma|\alpha|\gamma|\dots$ appears, a contradiction.

Case γ^3

We have $\gamma = \frac{2\pi}{3} < 2\alpha$. The AAD $|\gamma^\beta|^\beta|\gamma|\gamma|$ of γ^3 gives $|\beta|\beta|\dots$. Similar to the proof of Lemma 5, $\beta^2 \dots$ is not a vertex.

5.2 The vertex types of degree 4

If there is no vertices of degree 3, then $f_\Delta \geq 8$ by (2.3).

Case γ^4

We have $\gamma = \frac{\pi}{2} > \alpha$. By $\gamma^4 = |\gamma^\beta|^\beta|\gamma|\gamma|$ and similar proof of Lemma 5, we get $|\beta|\beta|\dots = \alpha\beta^3, \alpha\beta^2\gamma, \alpha^2\beta^2$.

Subcase $|\beta|\beta|\dots = \alpha\beta^3$, $\text{AVC} \subset \{\gamma^4, \alpha\beta^3\}$

There is no the vertex $\alpha\gamma \dots$, contradicting Lemma 1.

Subcase $|\beta|\beta|\dots = \alpha^2\beta^2$, $\text{AVC} \subset \{\gamma^4, \alpha^2\beta^2, \alpha\beta\gamma^2\}$

As shown in Figure 19, we get $\alpha^2\gamma \dots$, contradicting the AVC.

Subcase $|\beta|\beta|\dots = \alpha\beta^2\gamma$, $\text{AVC} \subset \{\gamma^4, \alpha\beta^2\gamma\}$

In Figure 25, γ^4 determines T_1, T_2, T_3, T_4 . By the symmetry of the partial tiling and $\beta^2 \dots = \alpha\beta^2\gamma$, we might as well take $|\beta_1|\beta_2|\dots = |\beta_1|\beta_2|\gamma|\alpha|$ which determines T_5, T_6 ; $|\beta_1|\beta_4|\dots = |\beta_1|\beta_4|\alpha|\gamma|$ determines T_7, T_8 . Similarly, we can determine T_9, \dots, T_{12} . Then $T_{13}, T_{14}, \dots, T_{32}$ are determined and the 3D picture is the 18th of Figure 4.

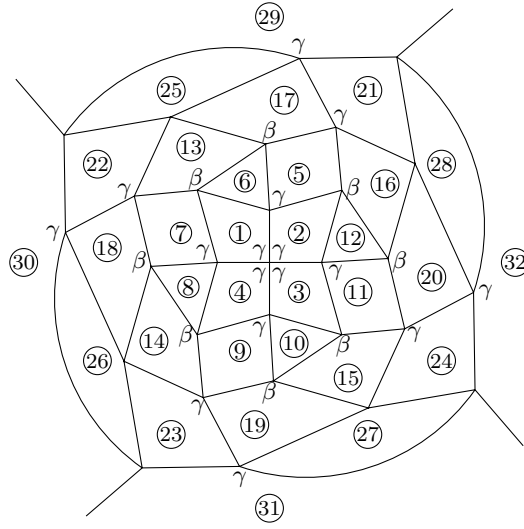


Figure 25: $T(8a^3, 24a^4; 24\alpha\beta^2\gamma, 6\gamma^4)$.

Case $\alpha^2\beta^2$

By $2\beta + 2\gamma > 2\pi = 2\alpha + 2\beta$, we have $\gamma > \alpha$. If there is a vertex $\alpha^2\beta^2 = |\alpha|\alpha|\beta|\beta|$, then we get $|\gamma|\gamma|\dots = \alpha\beta\gamma^2, \beta\gamma^3, \alpha^3\gamma^2, \alpha^2\gamma^3, \alpha\gamma^3, \alpha\gamma^4, \gamma^5$ by similar proof of Lemma 5.

$ \gamma \gamma \dots$	AVC \subset a set	Conclusion
$\beta\gamma^3$	$\{\alpha^2\beta^2, \beta\gamma^3\}$	No $\alpha\gamma\dots$, contradicting Lemma 1
γ^5	$\{\alpha^2\beta^2, \gamma^5\}$	

Table 6: The simple cases when $|\alpha|\alpha|\beta|\beta|$ appears.

Subcase $|\gamma|\gamma|\dots = \alpha\gamma^k (k = 3, 4)$, AVC $\subset \{\alpha^2\beta^2, \alpha\gamma^k\}$

By $\alpha\gamma^k = |\gamma|\gamma|\gamma|\dots$, we get $\alpha^2\gamma\dots$ as shown in Figure 19, contradicting the AVC.

Subcase $|\gamma|\gamma|\dots = \alpha^2\gamma^3$, AVC $\subset \{\alpha^2\beta^2, \alpha^2\gamma^3\}$

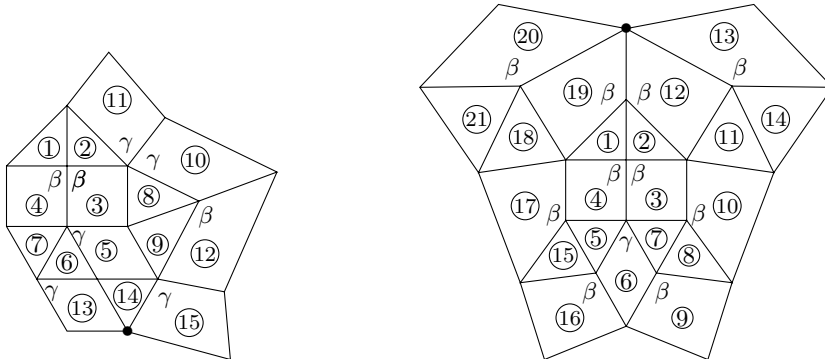


Figure 26: $|\gamma|\gamma|\dots = \alpha^2\gamma^3$.

In Figure 26, $|\alpha|\alpha|\beta|\beta|$ determines T_1, T_2, T_3, T_4 . When $|\gamma_4|\gamma_3|\dots = |\gamma_4|\gamma_3|\gamma|\alpha|\alpha|$, T_5, T_6, T_7

are determined in the first. Then we can determine T_8, \dots, T_{15} but $\alpha\beta\gamma\dots$ appears, contradicting the AVC. Therefore, $|\gamma_4|\gamma_3|\dots = |\gamma_4|\gamma_3|\alpha|\gamma|\alpha|$ determines T_5, T_6, T_7 in the second. Then we can determine T_8, \dots, T_{21} but $\gamma^4\dots$ appears, contradicting the AVC.

Subcase $|\gamma|\gamma|\dots = \alpha\beta\gamma^2$, $\text{AVC} \subset \{\alpha^2\beta^2, \alpha\beta\gamma^2\}$

In the first of Figure 27, $|\alpha|\alpha|\beta|\beta|$ determines T_1, T_2, T_3, T_4 . By the symmetry of the partial tiling and $\gamma^2\dots = \alpha\beta\gamma^2$, we might as well take $|\gamma_3|\gamma_4|\dots = |\gamma_3|\gamma_4|\alpha|\beta|$ which determines T_5, T_6 . Then we can determine T_7, T_8, \dots, T_{20} and the 3D picture is the 16th of Figure 4.

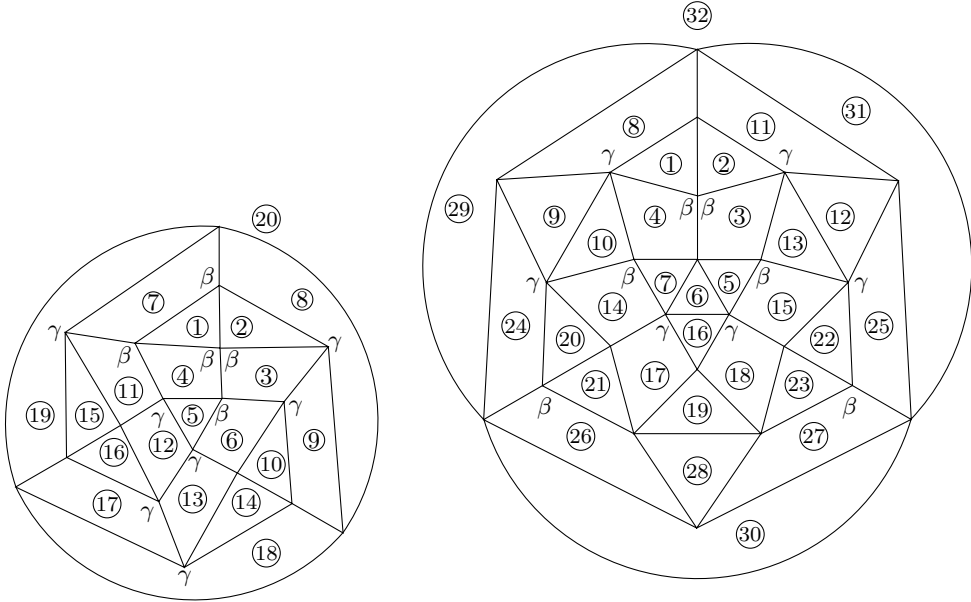


Figure 27: $|\gamma|\gamma|\dots = \alpha\beta\gamma^2, \alpha^3\gamma^2$.

Subcase $|\gamma|\gamma|\dots = \alpha^3\gamma^2$, $\text{AVC} \subset \{\alpha^2\beta^2, \alpha^3\gamma^2\}$

In the second of Figure 27, $|\alpha|\alpha|\beta|\beta|$ determines T_1, T_2, T_3, T_4 ; $\gamma^2\dots = \alpha^3\gamma^2$ determines T_5, T_6, T_7 . When $|\gamma_4|\alpha_1|\dots = |\gamma_4|\alpha_1|\alpha|\dots$, we get $|\alpha_2|\alpha_1|\alpha|\dots = |\alpha_2|\alpha_1|\alpha|\gamma|\gamma|$. But $|\beta|\alpha_2|\gamma_3|\dots$ appears, contradicting the AVC. So $|\gamma_4|\alpha_1|\dots = |\gamma_4|\alpha_1|\gamma|\alpha|\alpha|$ determines T_8, T_9, T_{10} . Then T_{11}, \dots, T_{32} are determined and the 3D picture is the 19th of Figure 4.

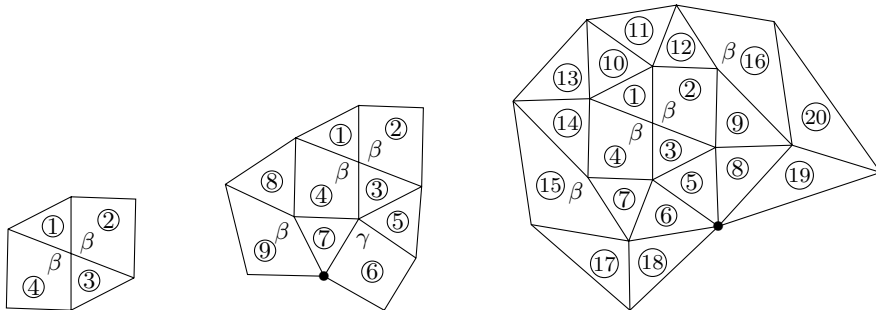


Figure 28: $\alpha^2\beta^2$ can only be $|\alpha|\beta|\alpha|\beta|$.

Now the vertex $\alpha^2\beta^2$ can only be $|\alpha|\beta|\alpha|\beta|$ which determines T_1, T_2, T_3, T_4 in Figure 28. By

similar proof of Lemma 5, we have $\beta^2 \cdots = \alpha^2 \beta^2$. So $|\beta|\beta|\cdots$ is not a vertex. Then $|\gamma|\gamma|\cdots$ can never be a vertex and $|\alpha\gamma|\cdots = |\alpha\gamma|\beta|\gamma|, |\alpha|\alpha\gamma|\alpha\gamma|, \alpha^4\gamma$.

When $|\alpha\gamma|\cdots = |\alpha\gamma|\beta|\gamma|$, we have the AVC $\subset \{|\alpha|\beta|\alpha|\beta|, |\alpha\gamma|\beta|\gamma|\}$. Then one of $|\alpha_3|\gamma_4|\cdots$ and $|\alpha_3|\gamma_2|\cdots$ must be $|\alpha\gamma|\gamma|\beta|$, contradicting the AVC.

When $|\alpha\gamma|\cdots = |\alpha|\alpha\gamma|\alpha\gamma|$, we have the AVC $\subset \{|\alpha|\beta|\alpha|\beta|, |\alpha|\alpha\gamma|\alpha\gamma|\}$. Then we can determine T_5, T_6, \dots, T_9 in the second of Figure 28. But $\alpha\beta\gamma\cdots$ appears, contradicting the AVC.

When $|\alpha\gamma|\cdots = \alpha^4\gamma$, we have the AVC $\subset \{|\alpha|\beta|\alpha|\beta|, \alpha^4\gamma\}$. Then we can determine T_5, \dots, T_{20} in the third of Figure 28. But $\alpha^5\cdots$ appears, contradicting the AVC.

Case $\alpha\gamma^3$

We have $\gamma > \frac{1}{2}\pi > \alpha$. The AAD $|\alpha\gamma^\beta|\beta|\gamma|\gamma|$ of $\alpha\gamma^3$ gives $|\beta|\beta|\cdots$. By similar proof of Lemma 5, $\beta^2\cdots$ is not a vertex.

Case $\alpha^2\gamma^2$

We have $\gamma > \frac{1}{2}\pi > \alpha$. By similar proof of Lemma 5, $\beta^2\cdots$ is not a vertex. So $|\gamma|\gamma|\cdots$ is not a vertex by Lemma 1. This implies $\alpha^2\gamma^2 = |\alpha\gamma|\alpha\gamma|$ which determines T_1, T_2, T_3, T_4 in Figure 29. Then we can get $|\alpha|\beta|\cdots = \alpha^3\beta$ and the AVC $\subset \{\alpha^2\gamma^2, \alpha^3\beta\}$. Then T_5, \dots, T_{11} are determined and the 3D picture is the 14th of Figure 4.

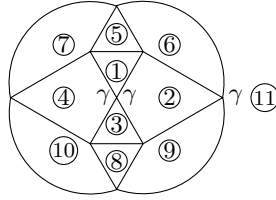


Figure 29: $T(8a^3, 3a^4; 6\alpha^3\beta, 3\alpha^2\gamma^2)$.

Case $\alpha\beta\gamma^2$

Similar to the proof of Lemma 5, $\beta^2\cdots$ is not a vertex. So $|\gamma|\gamma|\cdots$ can never be a vertex by Lemma 1. Then $\alpha\beta\gamma^2 = |\alpha\gamma|\beta|\gamma|$ determines T_1, T_2, T_3, T_4 in Figure 30. We can get $|\beta|\gamma|\cdots = |\beta|\gamma|\alpha\gamma|$ which determines T_5, \dots, T_{12} . Then $\alpha^2\beta\cdots = \alpha^4\beta$ determines T_{13}, \dots, T_{19} and the AVC $\subset \{\alpha\beta\gamma^2, \alpha^4\beta\}$. But $\alpha^5\cdots$ appears, contradicting the AVC.

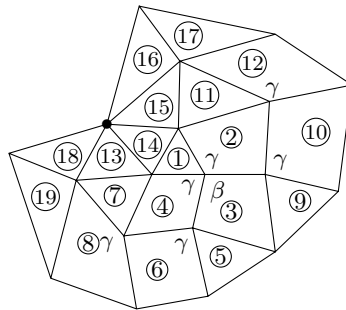


Figure 30: $\alpha\beta\gamma^2$ is a vertex.

Case $\alpha^3\gamma$

We have $\gamma > \frac{1}{2}\pi > \alpha$. Similar to the proof of Lemma 5, $\beta^2 \dots$ is not a vertex. So $|\gamma|\gamma|\dots$ can never be a vertex by Lemma 1. By $\alpha^3\gamma = |\gamma\beta|\alpha\alpha|\dots$, we get $|\alpha|\beta|\dots$ which is not a vertex.

Case $\beta\gamma^3$

We have $\gamma > \frac{1}{3}\pi$. Then the AAD $|\gamma\beta|\beta\gamma|\dots$ of $\beta\gamma^3$ gives $|\beta|\beta|\dots = \alpha\beta^3, \alpha\beta^2\gamma$.

Subcase $|\beta|\beta|\dots = \alpha\beta^3$, $\text{AVC} \subset \{\beta\gamma^3, \alpha\beta^3\}$

There is no the vertex $\alpha\gamma\dots$, contradicting Lemma 1.

Subcase $|\beta|\beta|\dots = \alpha\beta^2\gamma$, $\text{AVC} \subset \{\beta\gamma^3, \alpha\beta^2\gamma\}$

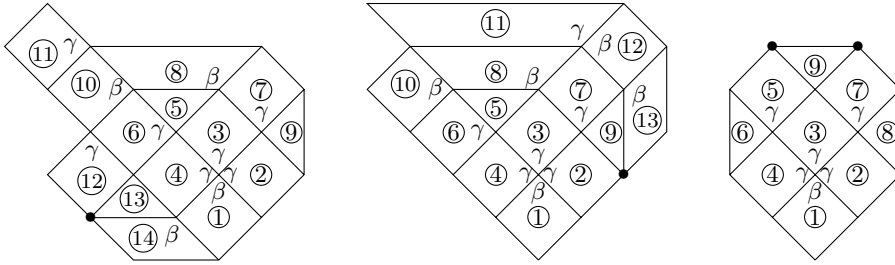


Figure 31: $|\beta|\beta|\dots = \alpha\beta^2\gamma$.

In Figure 31, $\beta\gamma^3$ determines T_1, T_2, T_3, T_4 . By the symmetry of the partial tiling and $\beta^2 \dots = \alpha\beta^2\gamma$, we might as well take $|\beta_3|\beta_4|\dots = |\gamma|\alpha|\beta_3|\beta_4|$ which determines T_5, T_6 in the first and second; $\alpha\gamma\dots = \alpha\beta^2\gamma$ determines T_7, T_8 ; $\beta^2\gamma\dots = \alpha\beta^2\gamma$ determines T_9 ; $\alpha\beta\gamma\dots = \alpha\beta^2\gamma$ determines T_{10} . When $|\gamma_7|\gamma_8|\dots = |\gamma_7|\gamma_8|\beta|\gamma|$, $|\beta_8|\gamma_{10}|\dots = \beta\gamma^3$ determines T_{11} in the first; $|\gamma_{10}|\gamma_6|\dots = |\gamma_{10}|\gamma_6|\gamma|\dots$ determines T_{12} ; $\beta^2\gamma\dots = \alpha\beta^2\gamma$ determines T_{13} ; $\alpha\beta\gamma\dots = \alpha\beta^2\gamma$ determines T_{14} . But $\alpha\gamma^2\dots$ appears, contradicting the AVC. So $|\gamma_7|\gamma_8|\dots = |\gamma_7|\gamma_8|\gamma|\beta|$ determines T_{11}, T_{12} in the second; $\alpha\beta\gamma\dots = \alpha\beta^2\gamma$ determines T_{13} . But $\alpha\gamma^2\dots$ appears, contradicting the AVC.

Therefore, $|\beta_3|\beta_4|\dots = |\alpha|\gamma|\beta_3|\beta_4|$ and $|\beta_3|\beta_2|\dots = |\alpha|\gamma|\beta_3|\beta_2|$ which determine T_5, \dots, T_8 in the third. Then T_9 is determined. But one of $|\alpha_9|\gamma_7|\dots$ and $|\alpha_9|\gamma_5|\dots$ can never be a vertex.

Case $\alpha\beta^3$

We have $\beta < \frac{5}{9}\pi$ and $\gamma > \frac{4}{9}\pi$. Then the AAD $|\alpha|\beta\gamma|\gamma\beta|\beta|$ of $\alpha\beta^3$ gives $|\gamma|\gamma|\dots = \alpha^3\gamma^2$ and the $\text{AVC} \subset \{\alpha\beta^3, \alpha^3\gamma^2\}$. Similar to Figure 19, $\alpha^2\beta\dots$ appears, contradicting the AVC.

Case $\alpha^2\beta\gamma$

By $2\alpha + 2\beta > 2\alpha + \beta + \gamma = 2\pi$, we get $\alpha + \beta > \pi$. Similar to the proof of Lemma 5, $\beta^2 \dots$ is not a vertex. So $|\gamma|\gamma|\dots$ can never be a vertex by Lemma 1. Then we have $\beta\gamma\dots = \alpha^2\beta\gamma$, $\alpha\beta\dots = \alpha^2\beta\gamma$.

If there is a vertex $\alpha^2\beta\gamma = |\alpha|\alpha|\beta|\gamma|$, then T_1, \dots, T_6 are determined in Figure 32. By the symmetry of the partial tiling and $\alpha\beta\dots = \alpha^2\beta\gamma$, we might as well take $|\beta_4|\alpha_1|\dots = |\beta_4|\alpha_1|\alpha|\gamma|$ which determines T_7, T_8 . Then we can determine T_9, \dots, T_{12} . Since $4\alpha < 2\pi$, T_{13} and T_{14} are determined when $5\alpha \leq 2\pi$. When $5\alpha < 2\pi$, $|\alpha_9|\alpha_5|\alpha_6|\alpha_{10}|\alpha_{13}|\dots$ is not a vertex. When $5\alpha = 2\pi$, we get a tiling in the second. By calculation, we have $\beta = 2\alpha = 2\gamma = \frac{4}{5}\pi$. Then the tiling is of the icosahedral type by Lemma 7. So $|\beta_4|\alpha_1|\dots = |\beta_4|\alpha_1|\gamma|\alpha|$ and $|\beta_3|\alpha_6|\dots = |\beta_3|\alpha_6|\gamma|\alpha|$. Then we get a tiling as the first of Figure 33, which is the same as the third of Figure 12.

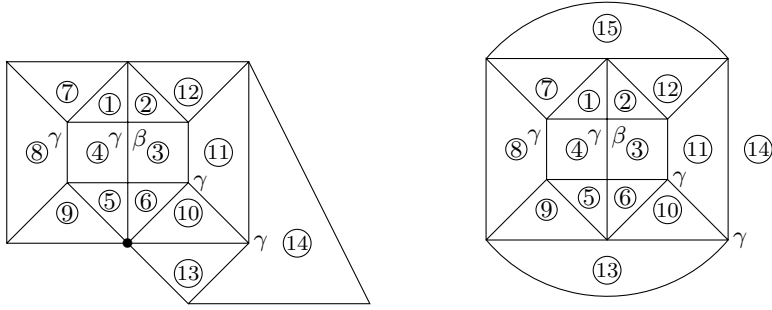


Figure 32: $|\alpha|\alpha|\beta|\gamma|$ appears.

Now $\alpha^2\beta\gamma$ can only be $|\alpha|\beta|\alpha|\gamma|$, and we get a tiling as the second of Figure 33 which is the same as the fourth of Figure 12. We notice that the red line divides the tilings into two same modules and the first tiling becomes the second by flipping one of the two modules.

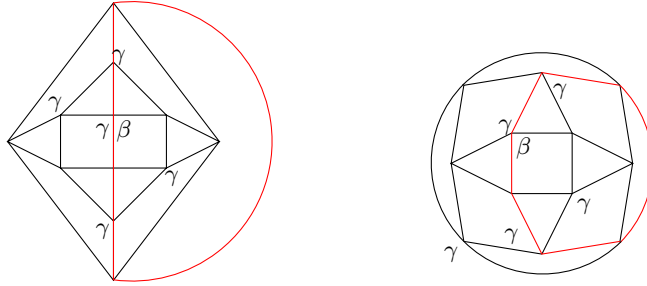


Figure 33: $T(8a^3, 6a^4; 12\alpha^2\beta\gamma)$.

Case $\alpha\beta^2\gamma$

By $2\beta + 2\gamma > 2\pi = \alpha + 2\beta + \gamma$, we get $\gamma > \alpha$. Similar to the proof of Lemma 5, we can get $\beta^2 \dots = \alpha\beta^2\gamma$ and $\beta\gamma \dots = \alpha\beta^2\gamma$. If there is a vertex $\alpha\beta^2\gamma = |\alpha|\beta\gamma|\gamma\beta|\gamma|$, then we get $|\gamma|\gamma| \dots = \gamma^5, \alpha\gamma^4, \alpha^2\gamma^3, \alpha^3\gamma^2$.

Subcase $|\gamma|\gamma| \dots = \gamma^5$, $AVC \subset \{\alpha\beta^2\gamma, \gamma^5\}$

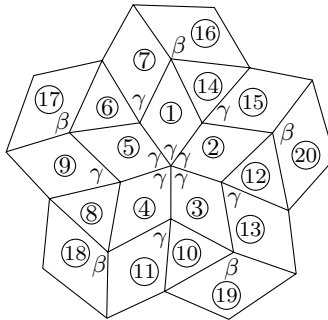


Figure 34: $T(20a^3, 60a^4; 60\alpha\beta^2\gamma, 12\gamma^5)$.

In Figure 34, γ^5 determines T_1, \dots, T_5 . By the symmetry of the partial tiling and $\beta^2 \dots =$

$\alpha\beta^2\gamma$, we might as well take $|\beta_1|\beta_5|\dots = |\beta_1|\beta_5|\alpha|\gamma|$ which determines T_6, T_7 . Then we can determine $T_8, \dots, T_{20}, \dots$ and we get a tiling whose 3D picture is the 23rd of Figure 4.

Subcase $|\gamma|\gamma|\dots = \alpha\gamma^4$, $AVC \subset \{\alpha\beta^2\gamma, \alpha\gamma^4\}$

The vertex $\alpha\gamma^4$ determines T_1, \dots, T_5 in Figure 35. By the symmetry of the partial tiling and $\alpha\beta\dots = \alpha\beta^2\gamma$, we might as well take $|\alpha_1|\beta_5|\dots = |\alpha_1|\beta_5|\beta|\gamma|$ which determines T_6, T_7 . Then T_8, \dots, T_{39} are determined. But $|\beta_{35}|\gamma_{36}|\gamma_{39}|\dots$ appears, contradicting the AVC.

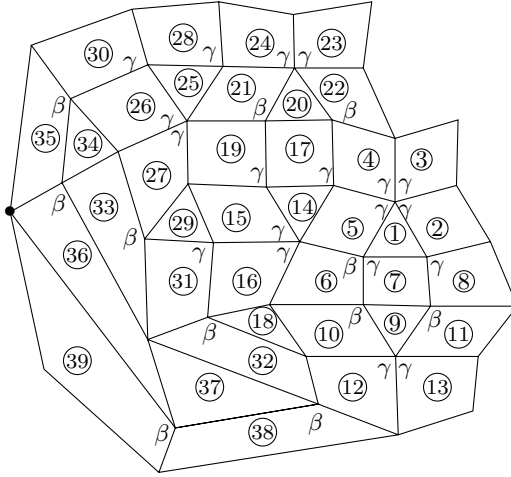


Figure 35: $|\gamma|\gamma|\dots = \alpha\gamma^4$.

Subcase $|\gamma|\gamma|\dots = \alpha^2\gamma^3$, $AVC \subset \{\alpha\beta^2\gamma, \alpha^2\gamma^3\}$

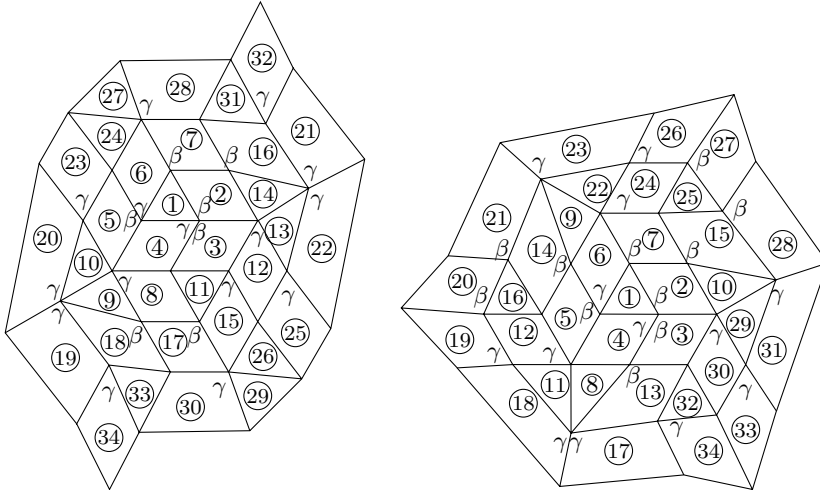


Figure 36: $\{20\alpha^3, 36\alpha^4; 36\alpha\beta^2\gamma, 12\alpha^2\gamma^3 : 2\}$.

In Figure 36, $|\alpha|\beta|\beta|\gamma|$ determines T_1, \dots, T_4 . When $|\alpha_1|\beta_4|\dots = |\alpha_1|\beta_4|\beta|\gamma|$, T_5, T_6, T_7 are determined. We see that the partial tiling is rotationally symmetric by rotating 120° around the center of T_1 . Then we have the following situations:

- $|\gamma_5|\gamma_4|\dots = |\gamma_5|\gamma_4|\gamma|\alpha|\alpha|$;

- $\gamma_5\gamma_4|\dots = \gamma_5\gamma_4|\alpha|\alpha|\gamma|, \gamma_7\gamma_6|\dots = \gamma_7\gamma_6|\alpha|\dots, \gamma_3\gamma_2|\dots = \gamma_3\gamma_2|\alpha|\dots;$
- $\gamma_5\gamma_4|\dots = \gamma_5\gamma_4|\alpha|\gamma|\alpha|, \gamma_7\gamma_6|\dots = \gamma_7\gamma_6|\alpha|\gamma|\alpha|, \gamma_3\gamma_2|\dots = \gamma_3\gamma_2|\alpha|\gamma|\alpha|.$

In situation 1, we can determine T_8, T_9, T_{10} in the first of Figure 36. Then T_{11}, \dots, T_{26} are determined. When $\gamma_7\gamma_6|\alpha_{24}|\dots = \gamma_7\gamma_6|\alpha_{24}|\gamma|\dots$, we get $|\beta|\alpha_{24}|\gamma_{23}|\dots = |\beta|\alpha_{24}|\gamma_{23}|\beta|$. But $\gamma|\beta_{23}|\gamma_{20}|\dots$ appears, contradicting the AVC. So $\gamma_7\gamma_6|\alpha_{24}|\dots = \gamma_7\gamma_6|\alpha_{24}|\alpha|\gamma|$ determines T_{27}, T_{28} . Similarly, T_{29}, T_{30} are determined. Then we can get a tiling and the 3D picture is the 27th of Figure 4.

In situation 2, we can determine T_8, T_9, \dots, T_{12} in the second of Figure 36. Similarly, we get a different tiling and the 3D picture is the 28th of Figure 4.

In situation 3, we can determine T_8, \dots, T_{13} in the first of Figure 37. Then T_{14}, T_{15}, T_{16} are determined. But $\beta\gamma^2|\dots$ appears, contradicting the AVC.

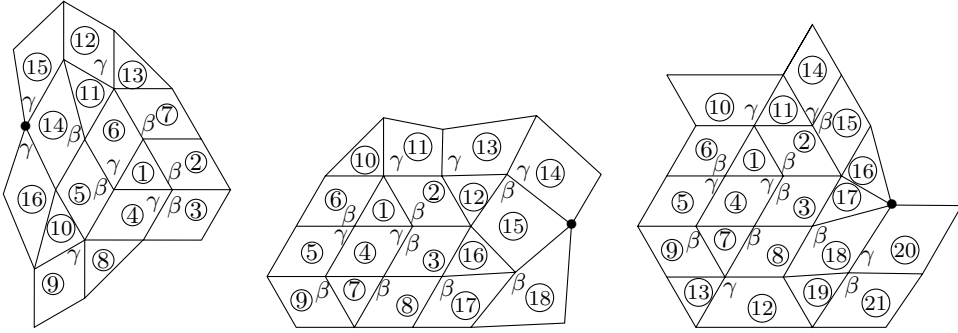


Figure 37: $|\gamma|\gamma|\dots = \alpha^2\gamma^3$.

When $|\alpha_1|\beta_4|\dots$ can only be $|\alpha_1|\beta_4|\gamma|\beta|$, T_5, T_6, \dots, T_9 are determined in the second and third of Figure 37. By the symmetry of the partial tiling, we might as well take $|\gamma_2|\alpha_1|\gamma_6|\dots = |\gamma_2|\alpha_1|\gamma_6|\alpha|\gamma|$. Then we can determine $T_{10}, T_{11}, \dots, T_{18}$ in the second. But $\beta\gamma^2|\dots$ appears, contradicting the AVC. Hence $|\gamma_2|\alpha_1|\gamma_6|\dots = |\gamma_2|\alpha_1|\gamma_6|\gamma|\alpha|$ and $|\gamma_9|\alpha_7|\gamma_8|\dots = |\gamma_9|\alpha_7|\gamma_8|\gamma|\alpha|$. Then we can determine T_{10}, \dots, T_{19} in the third. Since the partial tiling $\{T_{19}, T_{12}, T_8, T_{18}\}$ appears, $|\alpha_{19}|\beta_{18}|\dots = |\alpha_{19}|\beta_{18}|\gamma|\beta|$ determines T_{20}, T_{21} . But $\alpha^2\beta\gamma|\dots$ appears, contradicting the AVC.

Subcase $|\gamma|\gamma|\dots = \alpha^3\gamma^2$, $\text{AVC} \subset \{\alpha\beta^2\gamma, \alpha^3\gamma^2\}$

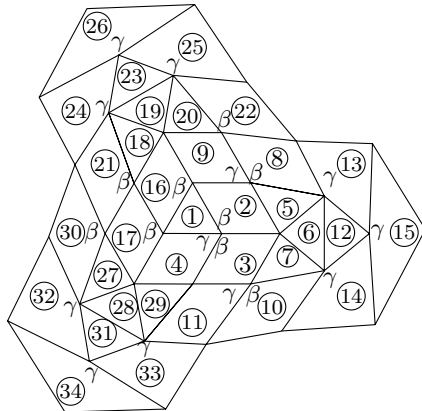


Figure 38: $T(20\alpha^3, 24\alpha^4; 24\alpha\beta^2\gamma, 12\alpha^3\gamma^2)$.

In Figure 38, $|\alpha|\beta|\beta|\gamma|$ determines T_1, \dots, T_4 , $\gamma^2 \dots = \alpha^3\gamma^2$ determines T_5, T_6, T_7 , etc. Then we get a tiling and the 3D picture is the 21st of Figure 4.

Now $\alpha\beta^2\gamma$ can only be $|\alpha|\beta|\gamma|\beta|$ which determines T_1, \dots, T_{13} in Figure 39. Similar to the proof of Lemma 5, we can get $\alpha^3\gamma \dots = \alpha^3\gamma^2, \alpha^4\gamma$. When $|\alpha_{12}|\gamma_7|\alpha_8|\alpha_{13}| \dots = \alpha^3\gamma^2$, we get $|\gamma_{11}|\alpha_{12}|\beta| \dots = |\gamma_{11}|\alpha_{12}|\beta|\beta|$, a contradiction. So $|\alpha_{12}|\gamma_7|\alpha_8|\alpha_{13}| \dots = \alpha^4\gamma$ and $|\alpha_6|\gamma_3|\alpha_8|\alpha_{13}| \dots = \alpha^4\gamma$ determine T_{14}, T_{15} , and we get the AVC $\subset \{\alpha\beta^2\gamma, \alpha^4\gamma\}$. But $|\alpha_{14}|\alpha_{13}|\alpha_{15}| \dots$ is not a vertex.

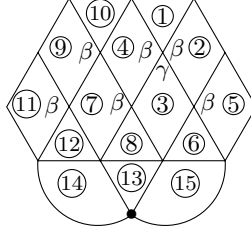


Figure 39: $\alpha\beta^2\gamma$ can only be $|\alpha|\beta|\gamma|\beta|$.

Case $\alpha^3\beta$

By $\alpha < \frac{\pi}{2}$, we have $\alpha + \beta > \pi$. Similar to the proof of Lemma 5, $\beta^2 \dots$ is not a vertex. So $|\gamma|\gamma| \dots$ can never be a vertex by Lemma 1, and $\alpha^2 \dots = \alpha^3\beta, \alpha^2\beta\gamma^2, \alpha^2\beta\gamma^3, \alpha^5\gamma^k (1 \leq k \leq 5), \alpha^4\gamma^k (2 \leq k \leq 4), \alpha^3\gamma^3$. Obviously $|\alpha|\alpha|\beta| \dots$ can only be $|\alpha|\alpha|\alpha|\beta|$. As shown in figure 15, when $|\gamma|\alpha|\gamma| \dots$ appears, we get two $|\alpha|\beta| \dots$ which are $|\alpha|\alpha|\alpha|\beta|$.

In the left of Figure 40, $\alpha^3\beta$ determines T_1, \dots, T_4 . When $|\alpha_3|\alpha_2| \dots = |\alpha_3|\alpha_2|\gamma| \dots$, T_5 is determined, and $|\beta_5|\alpha_2|\gamma_1| \dots = |\beta_5|\alpha_2|\gamma_1|\alpha| \dots = |\beta_5|\alpha_2|\gamma_1|\alpha|\gamma|$ determines T_6, T_7 . Then we get the AVC $\subset \{\alpha^3\beta, \alpha^2\beta\gamma^2\}$ which determines T_8, \dots, T_{13} . But $\alpha^3\gamma \dots$ appears, contradicting the AVC. So $|\alpha_3|\alpha_2| \dots \neq |\alpha_3|\alpha_2|\gamma| \dots$, $|\alpha_3|\alpha_4| \dots \neq |\alpha_3|\alpha_4|\gamma| \dots$ and they are $\alpha^4\gamma^2, \alpha^5\gamma, \alpha^5\gamma^2, \alpha^5\gamma^3, \alpha^3\beta$.

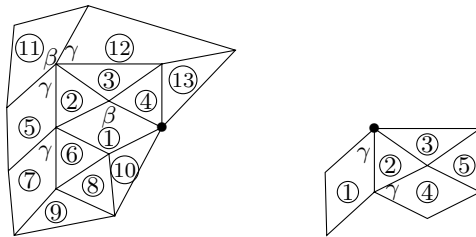


Figure 40: $|\alpha_3|\alpha_2| \dots = |\alpha_3|\alpha_2|\gamma| \dots$ or $|\gamma|\alpha|\alpha| \dots$ appears.

If $|\gamma|\alpha|\alpha| \dots$ appears, then T_1, T_2, T_3 are determined in the right of Figure 40. When $|\beta_1|\alpha_2| \dots = |\beta_1|\alpha_2|\gamma| \dots$, T_4, T_5 are determined, a contradiction. So $|\beta_1|\alpha_2| \dots = |\beta_1|\alpha_2|\alpha| \dots = |\beta_1|\alpha_2|\alpha|\alpha|$.

Subcase $|\alpha_3|\alpha_2| \dots = \alpha^4\gamma^2$, AVC $\subset \{\alpha^3\beta, \alpha^4\gamma^2\}$

The vertex $|\alpha_3|\alpha_2| \dots = |\alpha_3|\alpha_2|\alpha|\gamma|\alpha|\gamma|$ determines T_5, \dots, T_8 in Figure 41. Then we can determine T_9, \dots, T_{26} and the 3D picture is the 17th of Figure 4.

Subcase $|\alpha_3|\alpha_2| \dots = \alpha^5\gamma$, AVC $\subset \{\alpha^3\beta, \alpha^5\gamma\}$

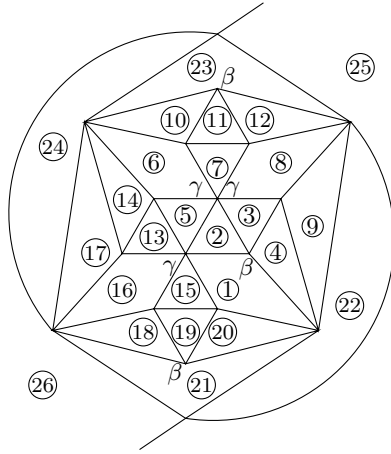


Figure 41: $T(20a^3, 6a^4; 12\alpha^3\beta, 6\alpha^4\gamma^2)$.

In the left of Figure 42, $\alpha^5\gamma$ determines T_1, \dots, T_6 ; $\alpha\beta \dots = \alpha^3\beta$ determines T_7, \dots, T_{10} ; $\alpha^2\gamma \dots = \alpha^5\gamma$ determines T_{11}, T_{12}, T_{13} . By the symmetry of the partial tiling, we have the following situations:

- $|\alpha_7|\alpha_8|\alpha_{13}| \dots = |\alpha_7|\alpha_8|\alpha_{13}|\beta|$ and $|\alpha_9|\alpha_{10}|\alpha_{11}| \dots = |\alpha_9|\alpha_{10}|\alpha_{11}|\beta|$;
- $|\alpha_7|\alpha_8|\alpha_{13}| \dots = |\alpha_7|\alpha_8|\alpha_{13}|\beta|$ and $|\alpha_9|\alpha_{10}|\alpha_{11}| \dots = |\alpha_9|\alpha_{10}|\alpha_{11}|\gamma|\alpha|\alpha|$;
- $|\alpha_7|\alpha_8|\alpha_{13}| \dots = |\alpha_7|\alpha_8|\alpha_{13}|\beta|$ and $|\alpha_9|\alpha_{10}|\alpha_{11}| \dots = |\alpha_9|\alpha_{10}|\alpha_{11}|\alpha|\gamma|\alpha|$;
- $|\alpha_7|\alpha_8|\alpha_{13}| \dots = |\alpha_7|\alpha_8|\alpha_{13}|\beta|$ and $|\alpha_9|\alpha_{10}|\alpha_{11}| \dots = |\alpha_9|\alpha_{10}|\alpha_{11}|\alpha|\alpha|\gamma|$;
- $|\alpha_7|\alpha_8|\alpha_{13}| \dots, |\alpha_7|\alpha_2|\alpha_3| \dots, |\alpha_9|\alpha_{10}|\alpha_{11}| \dots, |\alpha_9|\alpha_6|\alpha_5| \dots$ are not $\alpha^3\beta$.

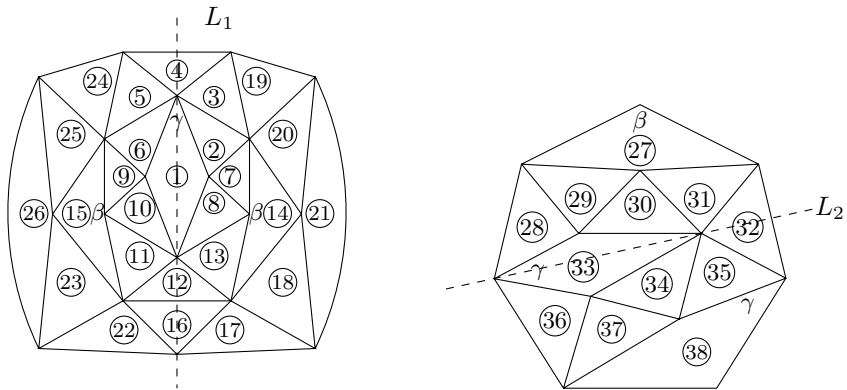


Figure 42: $|\alpha_7|\alpha_8|\alpha_{13}| \dots = \alpha^3\beta$ and $|\alpha_9|\alpha_{10}|\alpha_{11}| \dots = \alpha^3\beta$.

In situation 1, we can determine $T_{14}, T_{15}, \dots, T_{26}$ and the partial tiling is symmetric with respect to line L_1 . The rest of the region is a regular heptagon of angle β . By $\beta = 2\alpha + \gamma$, it is not difficult to find that the tiling of the regular heptagon is unique as the right of Figure 42 which is symmetric with respect to line L_2 . Therefore, we get four different tilings and the 3D pictures are the 29th through the 32nd in Figure 4.

In situation 2, we can determine T_{14}, \dots, T_{27} in Figure 43. By $|\alpha_{23}|\alpha_{22}|\alpha_{21}| \dots \neq |\alpha_{23}|\alpha_{22}|\alpha_{21}|\beta|$, we can get a new tiling whose 3D picture is the 33rd of Figure 4.

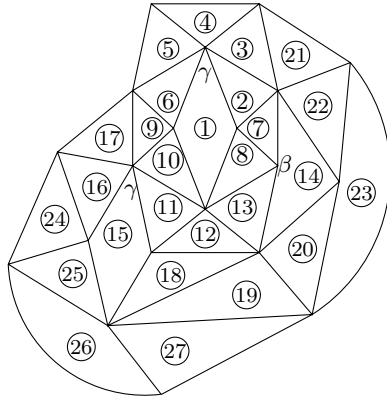


Figure 43: $|\alpha_7|\alpha_8|\alpha_{13}| \dots = \alpha^3\beta$ and $|\alpha_9|\alpha_{10}|\alpha_{11}| \dots = |\alpha_9|\alpha_{10}|\alpha_{11}|\gamma|\alpha|\alpha|$.

In situation 3, we can determine T_{14}, \dots, T_{29} as the first of Figure 44. But it is the same as the left of Figure 42.

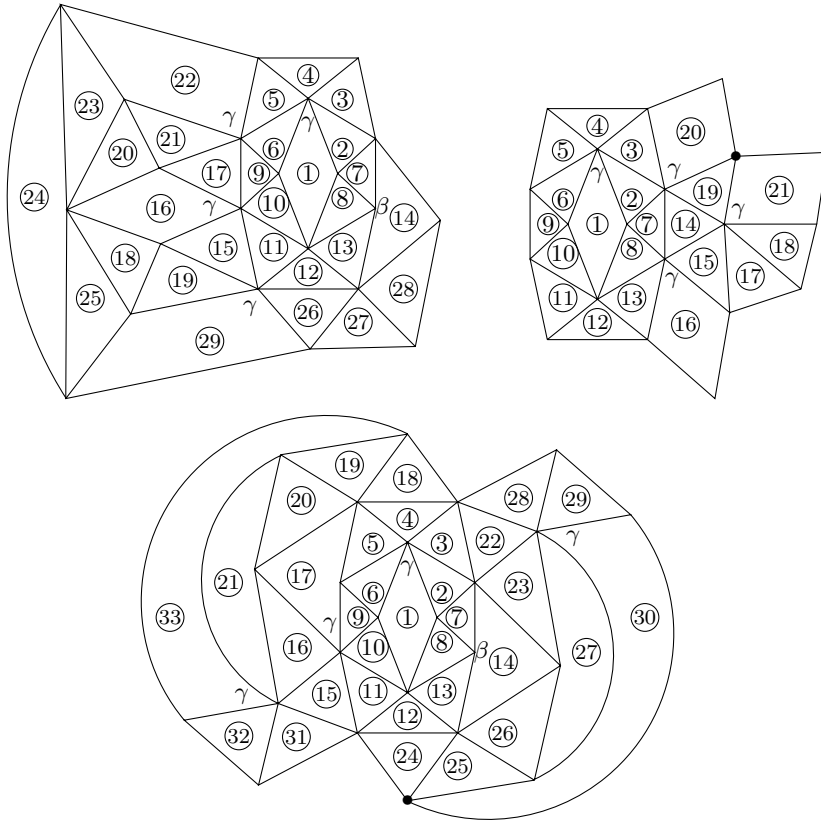


Figure 44: The other situations of $|\alpha_3|\alpha_2| \dots = \alpha^5\gamma$.

In situation 4, we can determine T_{14}, \dots, T_{27} as the third of Figure 44. Then $|\alpha_{27}|\alpha_{23}|\alpha_{22}| \dots$

$= |\alpha_{27}\alpha_{23}\alpha_{22}\alpha\alpha\gamma|$ and $|\alpha_{21}\alpha_{16}\alpha_{15}|\cdots = |\alpha_{21}\alpha_{16}\alpha_{15}\alpha\alpha\gamma|$ determine T_{28}, \dots, T_{33} . But $|\alpha_{24}\alpha_{25}\alpha_{30}|\cdots$ is not a vertex.

In situation 5, we can determine T_{14} as the second of Figure 44. If $|\alpha_{14}\alpha_7\alpha_8\alpha_{13}|\cdots = |\alpha\gamma\alpha_{14}\alpha_7\alpha_8\alpha_{13}|$ and $|\alpha_{14}\alpha_7\alpha_2\alpha_3|\cdots = |\alpha\gamma\alpha_{14}\alpha_7\alpha_2\alpha_3|$, then $\alpha_{14}\beta^2\cdots$ appears, a contradiction. So we might as well take $|\alpha_{14}\alpha_7\alpha_8\alpha_{13}|\cdots = |\gamma\alpha\alpha_{14}\alpha_7\alpha_8\alpha_{13}|$ which determines T_{15}, \dots, T_{21} . But $\alpha\beta^2\cdots$ appears, a contradiction.

Subcase $|\alpha_3\alpha_2|\cdots = \alpha^5\gamma^2$, $AVC \subset \{\alpha^3\beta, \alpha^5\gamma^2\}$

The vertex $|\alpha_3\alpha_2|\cdots$ is $|\alpha_3\alpha_2\alpha\gamma\alpha\gamma\alpha|$, $|\alpha_3\alpha_2\alpha\gamma\alpha\alpha\gamma|$ or $|\alpha_3\alpha_2\alpha\alpha\gamma\alpha\gamma|$. When $|\alpha_3\alpha_2|\cdots = |\alpha_3\alpha_2\alpha\gamma\alpha\gamma\alpha|$, T_5, \dots, T_{14} are determined as the left of Figure 45, contradicting $|\alpha_3\alpha_4|\cdots \neq |\alpha_3\alpha_4\gamma|\cdots$. When $|\alpha_3\alpha_2|\cdots = |\alpha_3\alpha_2\alpha\gamma\alpha\alpha\gamma|$, T_5, \dots, T_{23} are determined as the right of Figure 45. But $|\alpha_{10}\alpha_4\gamma_1\alpha_{13}\alpha_{23}|\cdots$ is not a vertex.

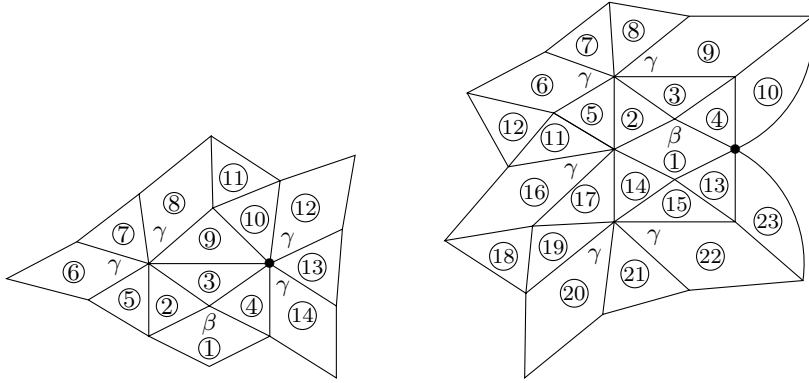


Figure 45: $|\alpha_3\alpha_2|\cdots$ is $|\alpha_3\alpha_2\alpha\gamma\alpha\gamma\alpha|$ or $|\alpha_3\alpha_2\alpha\gamma\alpha\alpha\gamma|$.

Hence $|\alpha_3\alpha_2|\cdots = |\alpha_3\alpha_2\alpha\alpha\gamma\alpha\gamma|$ determines T_5, \dots, T_9 in Figure 46. Then we can get a tiling and the 3D picture is the 22nd of Figure 4.

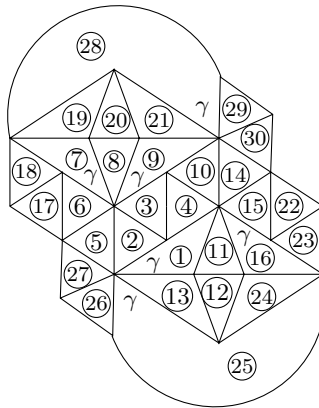


Figure 46: $T(44\alpha^3, 12\alpha^4; 24\alpha^3\beta, 12\alpha^5\gamma^2)$.

Subcase $|\alpha_3\alpha_2|\cdots = \alpha^5\gamma^3$, $AVC \subset \{\alpha^3\beta, \alpha^5\gamma^3\}$

The vertex $|\alpha_3\alpha_2|\cdots = |\alpha_3\alpha_2\alpha\gamma\alpha\gamma\alpha\gamma|$ determines T_5, \dots, T_{10} in Figure 47. Then T_{11}, \dots, T_{30} are determined. When $|\alpha_{29}\alpha_{28}|\cdots = \alpha^5\gamma^3$, $|\alpha_{29}\alpha_{28}\alpha\gamma\alpha\gamma\alpha\gamma|$ will appear,

contradicting $|\alpha_{29}\alpha_{28}| \cdots = |\alpha_{30}\alpha_{29}\alpha_{28}| \cdots$. So $|\alpha_{29}\alpha_{28}| \cdots = \alpha^3\beta$. Similarly we have $|\alpha_{21}\alpha_{22}| \cdots = \alpha^3\beta$. But $|\gamma|\alpha_{30}|\gamma_{27}|\alpha_{19}|\gamma_{16}|\alpha_{20}|\gamma| \cdots$ appears, contradicting the AVC.

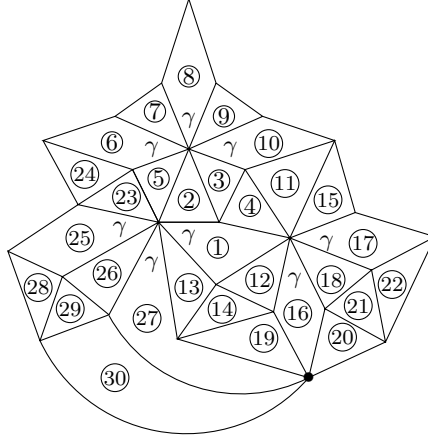


Figure 47: $|\alpha_3|\alpha_2| \cdots = \alpha^5\gamma^3$.

Now $|\alpha_3|\alpha_2| \cdots$ and $|\alpha_3|\alpha_4| \cdots$ can only be $\alpha^3\beta$, which determines T_5, T_6, T_7 in Figure 48. Then we get $|\gamma|\alpha|\gamma| \cdots = \alpha^2\beta\gamma^2, \alpha^2\beta\gamma^3, \alpha^5\gamma^k (2 \leq k \leq 5), \alpha^4\gamma^k (2 \leq k \leq 4), \alpha^3\gamma^3$.

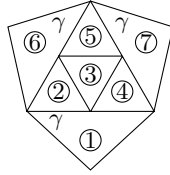


Figure 48: $|\alpha_3|\alpha_2| \cdots = \alpha^3\beta$ and $|\alpha_3|\alpha_4| \cdots = \alpha^3\beta$.

Subcase $|\gamma|\alpha|\gamma| \cdots = \alpha^2\beta\gamma^2$, $\text{AVC} \subset \{\alpha^3\beta, \alpha^2\beta\gamma^2\}$

We might as well take $|\gamma_6|\alpha_5|\gamma_7| \cdots = |\gamma_6|\alpha_5|\gamma_7|\beta|\alpha|$ which determines T_8, T_9 in the first of Figure 49. If $|\alpha_8|\beta_6| \cdots = |\alpha_8|\beta_6|\alpha| \cdots$, then $|\alpha_8|\beta_6| \cdots = |\alpha_8|\beta_6|\alpha|\alpha|$. But $|\alpha|\alpha_8|\gamma_9| \cdots$ appears, a contradiction. So $|\gamma_1|\alpha_2|\gamma_6| \cdots = |\gamma_1|\alpha_2|\gamma_6|\beta|\alpha|$ determines T_{10}, T_{11} . Similarly, T_{12}, T_{13} are determined. Then we can determine T_{14}, \dots, T_{32} and the 3D picture is the 20th of Figure 4.

Subcase $|\gamma|\alpha|\gamma| \cdots = \alpha^k\gamma^k (k = 3, 4, 5)$, $\text{AVC} \subset \{\alpha^3\beta, \alpha^k\gamma^k\}$

The vertex $\alpha^k\gamma^k$ can only be $|\gamma|\alpha|\gamma|\alpha| \cdots |\gamma|\alpha|$. When $k = 3$, we can determine T_8, \dots, T_{22} in the second of Figure 49 and the 3D picture is the 24th of Figure 4. When $k = 4, 5$, we have the same tilings and the 3D pictures respectively are the 25th and 26th of Figure 4.

Subcase $|\gamma|\alpha|\gamma| \cdots = \alpha^2\beta\gamma^3$, $\text{AVC} \subset \{\alpha^3\beta, \alpha^2\beta\gamma^3\}$

We might as well take $|\gamma_6|\alpha_5|\gamma_7| \cdots = |\gamma_6|\alpha_5|\gamma_7|\beta|\gamma|\alpha|$ which determines T_8, T_9, T_{10} in the first of Figure 50. Then T_{11}, \dots, T_{22} are determined. But $|\alpha_{19}|\gamma_6|\alpha_2|\gamma_1|\alpha_{21}| \cdots$ appears, contradicting the AVC.

Subcase $|\gamma|\alpha|\gamma| \cdots$ is others

There must be $|\gamma|\alpha|\alpha| \cdots$, which determines T_1, T_2, T_3 in the second of Figure 50. Then we can determine T_4, T_5 . But $|\alpha_4|\alpha_2| \cdots \neq |\alpha_4|\alpha_2|\beta|\alpha|$, a contradiction.

5.3 The vertex types of degree 5

Similar to the proof of Lemma 5, $\beta^2 \cdots$ can never be a vertex. So $|\gamma|\gamma|\cdots$ can never be a vertex by Lemma 1. This implies that $\gamma^5, \beta\gamma^4, \alpha\gamma^4, \alpha^2\gamma^3$ or $\alpha\beta\gamma^3$ can never be a vertex.

Case α^5

In Figure 51, α^5 determines T_1, \dots, T_5 . By similar proof of Lemma 5, $|\alpha|\alpha|\beta|\cdots$ is not a vertex. Then $|\alpha_1|\alpha_2|\cdots = |\alpha|\alpha_1|\alpha_2|\alpha|\cdots = \alpha^5$ determines T_6, T_7, T_8 . Similarly, T_9, \dots, T_{20} are determined. But it is a monohedral tiling, a contradiction.

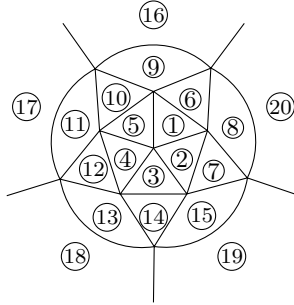


Figure 51: $T(20\alpha^3; 12\alpha^5)$.

Case $\alpha^3\gamma^2$

The vertex $\alpha^3\gamma^2 = |\alpha|\alpha|\gamma|\alpha|\gamma|$ determines T_1, \dots, T_5 in Figure 52. Similar to the proof of Lemma 5, $\alpha\beta \cdots = \alpha^4\beta$ determines T_6, \dots, T_{16} . Then we have the AVC $\subset \{\alpha^3\gamma^2, \alpha^4\beta\}$, and T_{17}, \dots, T_{34} are determined. But $\alpha^2\beta\gamma \cdots$ appears, contradicting the AVC.

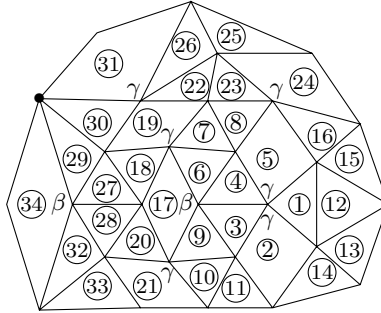


Figure 52: $\alpha^3\gamma^2$ is a vertex.

Case $\alpha^2\beta\gamma^2$

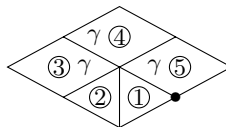


Figure 53: $\alpha^2\beta\gamma^2 = |\alpha|\alpha|\gamma|\beta|\gamma|$.

By $2\beta + 2\gamma > 2\pi$ and $3\alpha + \beta + \gamma > 2\pi$, we have $\beta > 2\alpha$ and $\alpha > \gamma$. Similar to the proof of Lemma 5, we get $\alpha^2\beta\cdots = \alpha^2\beta\gamma^2$. Then $|\alpha|\alpha|\beta|\cdots$ is not a vertex. When $|\gamma|\alpha|\gamma|\cdots$ appears, we get two $|\alpha|\beta|\cdots$ which are not vertices. So $\alpha^2\beta\gamma^2 = |\alpha|\alpha|\gamma|\beta|\gamma|$ determines T_1, \dots, T_5 in Figure 53. But $|\alpha_1|\beta_5|\cdots$ is not a vertex.

Case $\alpha^4\gamma$

By $2\alpha < \pi$, we have $2\alpha + \gamma > \pi$. The AAD $|\gamma^\beta|\alpha|\cdots$ of $\alpha^4\gamma$ gives $|\alpha|\beta|\cdots$. Similar to the proof of Lemma 5, $|\alpha|\beta|\cdots$ is not a vertex.

Case $\alpha^4\beta$

By $3\alpha + \beta + \gamma > 2\pi$, we have $\gamma > \alpha$. Similar to the proof of Lemma 5, $\alpha\beta\gamma\cdots$ and $\alpha^2\gamma\cdots$ can never be vertices. The AAD $|\beta^\gamma|\alpha|\cdots$ of $\alpha^4\beta$ gives $|\alpha|\gamma|\cdots$, which is not a vertex.

Appendix: Exact geometric data

(f_Δ, f_\diamond)	$\alpha, \beta, \gamma; \cos a = \cot \alpha \cot \frac{\alpha}{2} = \cot \frac{\beta}{2} \cot \frac{\gamma}{2}$	all vertices
(2, 3)	$\alpha \in [\arccos(\frac{1}{8}), \pi), \gamma = 2\pi - \alpha - \beta,$ $\beta = 2\operatorname{arccot} \left(-\frac{\sqrt{-8\cos\alpha+1}+2\cos\alpha-1}{2\sin\alpha} \right).$ When $\alpha = \arccos(\frac{1}{8})$, we have $\beta = \gamma = \arccos(-\frac{3}{4})$.	$6\alpha\beta\gamma$
(8, 6)	$\alpha \in [\arccos(\frac{1}{3}), \frac{1}{2}\pi), \gamma = 2\pi - 2\alpha - \beta,$ $\beta = 2\operatorname{arccot} \left(-\frac{\sin\alpha\sqrt{\frac{3\cos\alpha-1}{\cos\alpha-1}}+\cos(2\alpha)+\cos\alpha}{\sin(2\alpha)} \right).$ When $\alpha = \arccos(\frac{1}{3})$, we have $\beta = \gamma = \arccos(-\frac{1}{3})$.	$12\alpha^2\beta\gamma$

Table 7: Two 1-parameter families of protosets.

(f_Δ, f_\diamond)	$\alpha, \beta, \gamma; \cos a = \cot \alpha \cot \frac{\alpha}{2} = \cot \frac{\beta}{2} \cot \frac{\gamma}{2}$	all vertices
$(2, 6n - 3), n \geq 3$	$\gamma = 2\pi - 2\beta, \alpha = (1 - n)2\pi + (2n - 1)\beta,$ $\cos((2n - 1)\beta) = \frac{\cos\beta}{2\cos\beta-1}.$ $\lim_{n \rightarrow +\infty} \beta = \pi, \lim_{n \rightarrow +\infty} \gamma = 0,$ $\lim_{n \rightarrow +\infty} a = \frac{\pi}{3}, \lim_{n \rightarrow +\infty} \alpha = \arccos \frac{1}{3}.$	$6\alpha\beta\gamma^n, (6n - 6)\beta^2\gamma$

Table 8: A sequence of protosets.

(f_Δ, f_\diamond)	$\alpha, \beta, \gamma; \cos a = \cot \alpha \cot \frac{\alpha}{2} = \cot \frac{\beta}{2} \cot \frac{\gamma}{2}$	all vertices
(8, 2)	$\alpha = \frac{2\pi-\beta}{3}, \gamma = \beta,$ $\beta = 3 \arccos \left(\frac{1-\sqrt{2}+\sqrt{3+6\sqrt{2}}}{4} \right)$	$8\alpha^3\beta$
(32, 6)	$\alpha = \frac{2\pi-\beta}{4}, \gamma = \beta,$ $\beta = 4 \arcsin \left(\frac{(19+3\sqrt{33})^{\frac{2}{3}} - 2(19+3\sqrt{33})^{\frac{1}{3}} + 4}{6(19+3\sqrt{33})^{\frac{1}{3}}} \right)$	$24\alpha^4\beta$
(8, 18)	$\alpha = 2\pi - 3\beta, \gamma = \beta,$ $\beta = 2 \arctan \sqrt{7 - 4\sqrt{2}}$	$24\alpha\beta^3$
(4, 4)	$\alpha = 2\pi - 2\beta, \gamma = 2\beta - \pi,$ $\beta = \arccos(\frac{1-\sqrt{17}}{4})$	$4\alpha\beta^2, 4\alpha^2\gamma^2$
(8, 3)	$\alpha = \frac{2\pi-\beta}{3}, \gamma = \frac{\beta+\pi}{3},$ $\beta = 6 \arctan \left(\sqrt{3(9 - 4\sqrt{5})} \right)$	$6\alpha^3\beta, 3\alpha^2\gamma^2$
(4, 12)	$\alpha = \frac{4}{3}\pi - 2\gamma, \beta = \frac{2}{3}\pi,$ $\gamma = \arccos \left(\frac{c^{\frac{1}{6}}b^{\frac{1}{4}} - b^{\frac{3}{4}} + \sqrt{(-b+9c^{\frac{1}{3}})\sqrt{b+8\sqrt{c}}}}{4c^{\frac{1}{6}}b^{\frac{1}{4}}} \right)$ $c = 17 + 2\sqrt{41}, b = c^{\frac{2}{3}} + 3c^{\frac{1}{3}} + 5.$	$12\alpha\beta\gamma^2, 4\beta^3$
(8, 12)	$\alpha = \pi - \beta, \gamma = \frac{\pi}{2},$ $\beta = \arccos \left(-\frac{c^2+2c-14}{6c} \right)$ $c = (8 + 6\sqrt{78})^{\frac{1}{3}}.$	$6\alpha^2\beta^2, 12\alpha\beta\gamma^2$
(20, 6)	$\alpha = \frac{2\pi-\beta}{3}, \gamma = \frac{2\beta-\pi}{3},$ $\beta = -6 \arctan \left(3 + 2\sqrt{3} - \sqrt{24 + 14\sqrt{3}} \right)$	$12\alpha^3\beta, 6\alpha^4\gamma^2$
(8, 24)	$\gamma = \frac{\pi}{2}, \beta = \frac{3}{4}\pi - \frac{\alpha}{2},$ $\alpha = \arcsin \left(\frac{\sqrt{6}}{12} \left(b + \sqrt{\frac{-bc^2+12\sqrt{6}c-12b}{bc}} \right) \right)$ $c = (108 + 12\sqrt{69})^{\frac{1}{3}}, b = \sqrt{\frac{c^2+12}{c}}.$	$24\alpha\beta^2\gamma, 6\gamma^4$
(20, 12)	$\alpha = \pi - \beta, \gamma = \frac{3\beta-\pi}{2}, \beta = 2 \arcsin \left(\frac{1+\sqrt{33}}{8} \right)$	$12\alpha^2\beta^2, 12\alpha^3\gamma^2$

$(f_{\Delta}, f_{\diamond})$	$\alpha, \beta, \gamma; \cos a = \cot \alpha \cot \frac{\alpha}{2} = \cot \frac{\beta}{2} \cot \frac{\gamma}{2}$	all vertices
(20,12)	$\alpha = \frac{2\pi-\beta}{3}, \gamma = \frac{2\pi-\beta}{6},$ $\beta = \arcsin \left(\frac{\left(-3^{\frac{4}{3}} 2^{\frac{7}{12}} d^{\frac{1}{2}} - 3 \cdot 12^{\frac{1}{3}} b^{\frac{3}{2}} + 252 b^{\frac{1}{2}} c^{\frac{1}{6}} \right)^{\frac{1}{2}}}{12 b^{\frac{1}{4}} c^{\frac{1}{12}}} \right)$ $c = \frac{1597545 + 5291\sqrt{1689}}{\sqrt{(18c^2)^{\frac{1}{3}} + 120(12c)^{\frac{1}{3}} + 35592}},$ $b = \sqrt{(18c^2)^{\frac{1}{3}} + 120(12c)^{\frac{1}{3}} + 35592},$ $d = -35592 \cdot 2^{\frac{1}{6}} b + 240 \cdot 2^{\frac{5}{6}} b (3c)^{\frac{1}{3}} - \sqrt{2} b (9c^2)^{\frac{1}{3}} + 2340 \cdot 2^{\frac{1}{6}} \sqrt{c}.$	$12\alpha^3\beta, 12\alpha^2\beta\gamma^2$
(20,24)	$\alpha = 4\beta - 2\pi, \gamma = 4\pi - 6\beta, \cos \beta \in \left(-\frac{1}{2}, 0\right),$ $\cos \beta = \frac{\text{RootOf}(Z^6 + Z^5 - 4Z^4 - 3Z^3 + 3Z^2 - 1)}{2}.$	$24\alpha\beta^2\gamma, 12\alpha^3\gamma^2$
(44,12)	$\alpha = \frac{2\pi-\beta}{3}, \gamma = \frac{5\beta-4\pi}{6},$ $\beta = \arcsin \left(\frac{\left(-6\sqrt{3}b^{\frac{3}{4}} - 6d^{\frac{1}{2}} + 306b^{\frac{1}{4}}c^{\frac{1}{2}} \right)^{\frac{1}{2}}}{12b^{\frac{1}{8}}c^{\frac{1}{4}}} \right)$ $c = \left(38969189 + 564000\sqrt{1473} \right)^{\frac{1}{3}},$ $b = c^2 - 115c + 101641,$ $d = (-3b - 1035c)\sqrt{b} + 36576\sqrt{3c^3}.$	$24\alpha^3\beta, 12\alpha^5\gamma^2$
(20,60)	$\alpha = \frac{8}{5}\pi - 2\beta, \gamma = \frac{2}{5}\pi,$ $\beta = \arccos \left(\frac{\sqrt{6}(bd+33\sqrt{3}c^{\frac{3}{2}})^{\frac{1}{2}} + 3c^{\frac{1}{2}}d^{\frac{1}{2}} - \sqrt{3}d^{\frac{3}{2}}}{24c^{\frac{1}{2}}d^{\frac{1}{2}}} \right)$ $c = \left(-774\sqrt{5} + 10070 + 6\sqrt{85830 - 7890\sqrt{5}} \right)^{\frac{1}{3}},$ $b = -c^2 + 24\sqrt{5} + 43c - 460,$ $d = \sqrt{2c^2 + 43c - 48\sqrt{5} + 920}.$	$60\alpha\beta^2\gamma, 12\gamma^5$
(16,6)	$\alpha = \frac{2\pi-\beta}{3}, \gamma = \frac{\beta}{3}, \beta = \arcsin \left(\frac{\sqrt{bc}}{18c} \right)$ $c = \left(18559 + 3321\sqrt{-47} \right)^{\frac{1}{3}},$ $b = (\sqrt{-3} - 1)c^2 + 164c - 952 - 952\sqrt{-3}.$	$12\alpha^3\beta, 4\alpha^3\gamma^3$
(32,12)	$\alpha = \frac{2\pi-\beta}{3}, \gamma = \frac{2\beta-\pi}{6},$ $\beta = \arcsin \left(\frac{5-\sqrt{7}}{8} \right)$	$24\alpha^3\beta, 6\alpha^4\gamma^4$
(80,30)	$\alpha = \frac{2\pi-\beta}{3}, \gamma = \frac{5\beta-4\pi}{15},$ $\beta = \arcsin \left(\frac{(-2\sqrt{5}-6)\sqrt{5-2\sqrt{5}} + \sqrt{130-10\sqrt{5}}}{20} \right)$	$60\alpha^3\beta, 12\alpha^5\gamma^5$

(f_Δ, f_\diamond)	$\alpha, \beta, \gamma; \cos a = \cot \alpha \cot \frac{\alpha}{2} = \cot \frac{\beta}{2} \cot \frac{\gamma}{2}$	all vertices
(20,36)	$\alpha = 4\pi - 6\beta, \gamma = 4\beta - 2\pi,$ $\beta = \arcsin \left(\frac{(19516464 - 24642\sqrt{3}b + 111\sqrt{6}(bd+e)^{\frac{1}{2}})^{\frac{1}{2}}}{5328} \right)$ $c = (108 + 12\sqrt{849})^{\frac{1}{3}},$ $b = \sqrt{(-6\sqrt{849} + 54)c^2 + 1152c + 15552},$ $d = (5217\sqrt{3} + 2997\sqrt{283})c^2 + 3271392\sqrt{3} + (-223776\sqrt{3} + 10656\sqrt{283})c,$ $e = (147852\sqrt{849} - 1330668)c^2 - 28387584c + 766464768.$	$36\alpha\beta^2\gamma, 12\alpha^2\gamma^3$
(32,6)	$\alpha = \frac{2\pi - \beta}{3}, \gamma = \frac{5\beta - 4\pi}{3}, \beta = \arcsin \left(\frac{\sqrt{-3bc}}{6c} \right)$ $c = (-756 + 84\sqrt{-3})^{\frac{1}{3}},$ $b = (1 + \sqrt{-3})c^2 + 15c + 84 - 84\sqrt{-3}.$	$12\alpha^3\beta, 12\alpha^5\gamma$
(20,24)	$\alpha = 2\pi - 2\beta, \gamma = \frac{3}{2}\beta - \pi,$ $\beta = 4 \arccos \left(\frac{\sqrt{-3bc}}{12c} \right)$ $c = (28 + 84\sqrt{-3})^{\frac{1}{3}},$ $b = (1 + \sqrt{-3})c^2 - 32c + 28 - 28\sqrt{-3}.$	$(12 + k)\alpha\beta^2, k\alpha^3\gamma^4,$ $(24 - 2k)\alpha^2\beta\gamma^2$ $0 \leq k < 12$

Table 9: 20 sporadic protosets with some irrational angle.

References

- [1] C. Adams. The tiling book: An introduction to the mathematical theory of tilings. *Vol. 142. American Mathematical Society*, 2022.
- [2] C. Adams, C. Edgar, P. Hollander, L. Jacoby. The Rest of the Tilings of the Sphere by Regular Polygons. *preprint*, arXiv: 2101.10743, 2021.
- [3] Y. Akama, E. Wang, M. Yan. Tilings of sphere by congruent pentagons III: edge combination a^5 . *Adv. Math.*, 394 (2022), 107881.
- [4] J. H. Conway, A. J. Jones. Trigonometric diophantine equations (On vanishing sums of roots of unity). *Acta Arithmetica*, 30: 229-240, 1976.
- [5] H. M. Cheung, H. P. Luk, M. Yan. Tilings of the Sphere by Congruent Pentagons IV: Edge Combination a^4b . *preprint*, arXiv: 2307.11453, 2023.
- [6] B. Grünbaum, G. C. Shephard. Tilings and Patterns. W. H. Freeman and Dover, 1987 and 2016
- [7] K. S. Kedlaya, A. Kolpakov, B. Poonen, M. Rubinstein. Space vectors forming rational angles. *preprint*, arXiv: 2011.14232, 2020.
- [8] Y. Liao, P. Qian, E. Wang, Y. Xu. Tilings of the sphere by congruent quadrilaterals I: edge combination a^2bc . *preprint*, arXiv: 2110.10087, 2021.
- [9] Y. Liao, E. Wang. Tilings of the sphere by congruent quadrilaterals II: edge combination a^3b with rational angles. *preprint*, arXiv: 2205.14936, 2022.
- [10] Y. Liao, P. Qian, E. Wang, Y. Xu. Tilings of the sphere by congruent quadrilaterals III: edge combination a^3b with general angles. *preprint*, arXiv: 2206.15342, 2022.
- [11] Y. Sakano, Y. Akama. Anisohedral spherical triangles and classification of spherical tilings by congruent kites, darts and rhombi. *Hiroshima Mathematical Journal*, 2015, 45(3): 309-339.
- [12] D. M. Y. Sommerville. Division of space by congruent triangles and tetrahedra. *Proc. Royal Soc. Edinburgh*, 43:85–116, 1924.
- [13] Y. Ueno, Y. Agaoka. Classification of tilings of the 2-dimensional sphere by congruent triangles. *Hiroshima Math. J.*, 32(3):463–540, 2002.
- [14] E. Wang, M. Yan. Tilings of the sphere by congruent pentagons I: edge combinations a^2b^2c and a^3bc . *Adv. Math.*, 394 (2022), 107866.
- [15] E. Wang, M. Yan. Tilings of the sphere by congruent pentagons II: edge combination a^3b^2 . *Adv. Math.*, 394 (2022), 107867
- [16] E. Wang, M. Yan. Moduli of pentagonal subdivision tiling. *preprint*, arXiv: 1907.08776, 2019.